LIFE ON A YOUNG PLANET

THE FIRST THREE BILLION YEARS OF EVOLUTION ON EARTH

BY ANDREW H. KNOLL

Contents

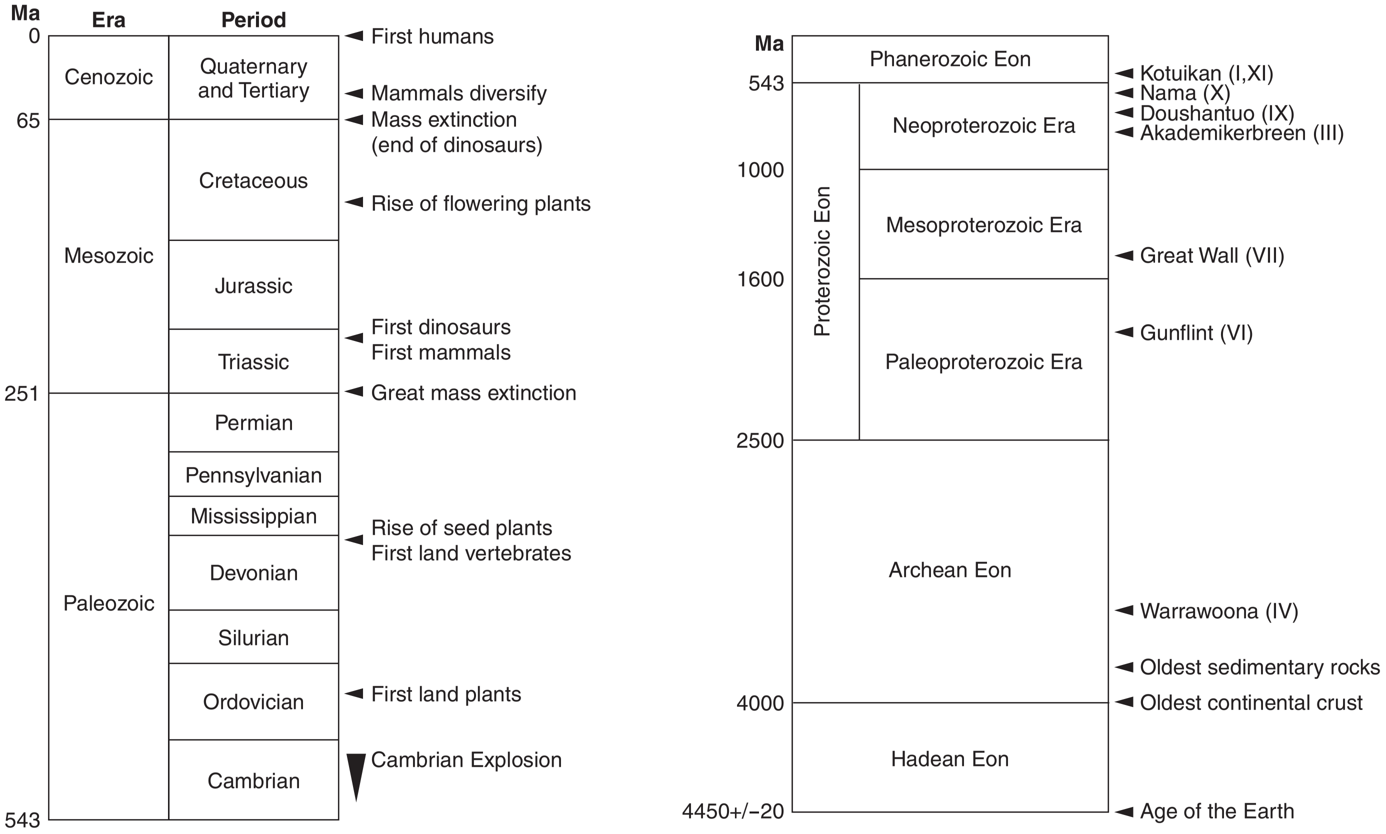

Figure P.1. The geologic timescale, showing the time relationships of major events in Phanerozoic evolution and the Precambrian rock units discussed in this book. (Ma = million years before present)

Figure 1.1. Fossiliferous cliffs along the Kotuikan River in Siberia. The distance from river level to the top of the cliff is more than 300 feet, recording some 20 million years of Early Cambrian history.

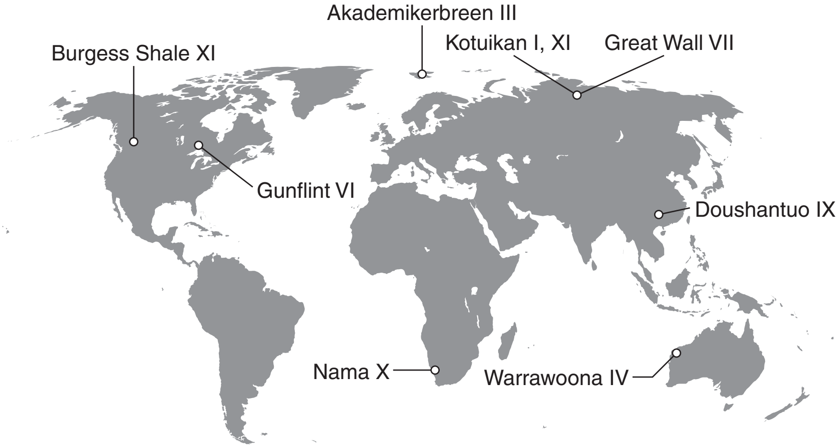

Figure 1.2. Map showing the location of the Kotuikan cliffs, along with principal localities discussed in subsequent chapters (denoted by roman numerals).

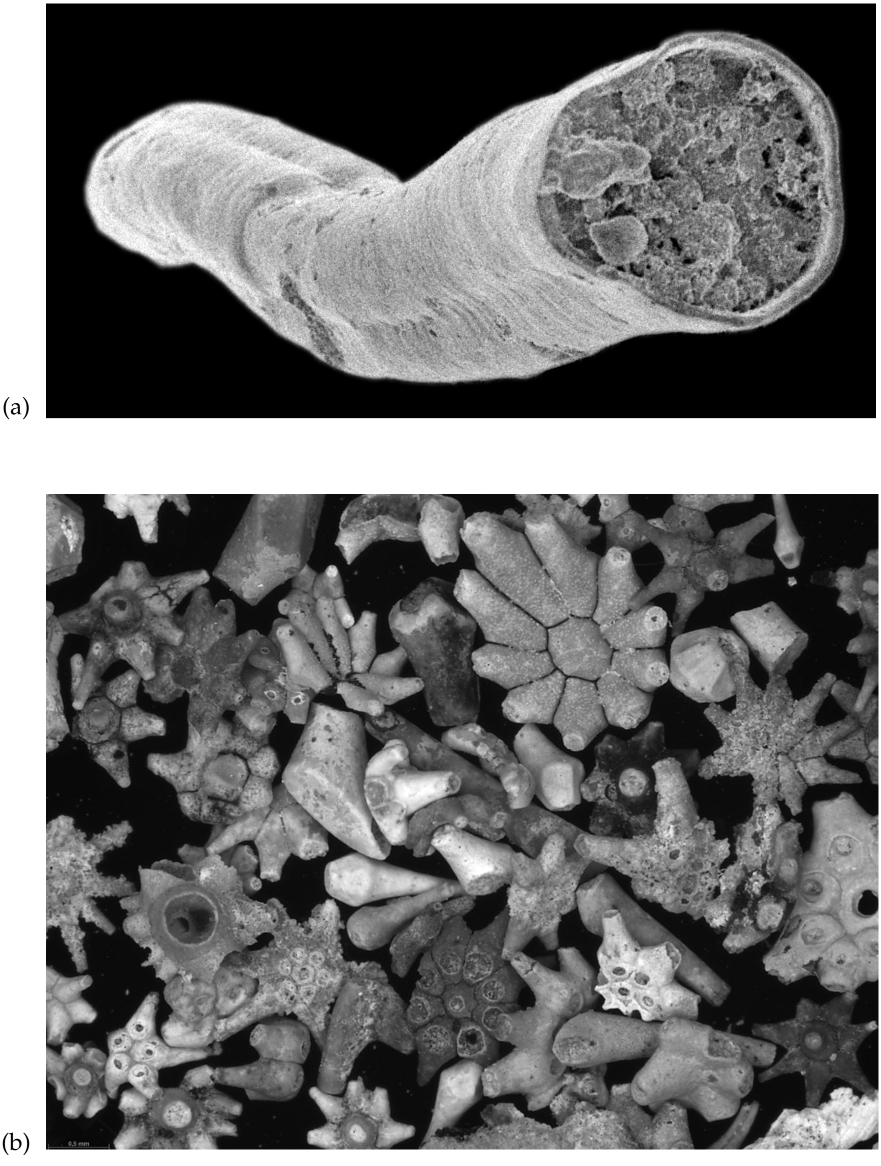

Figure 1.3. Small shelly fossils in basal Cambrian rocks. (a) *Anabarites trisulcatus*, the tiny skeletons found in lowermost Cambrian beds along the Kotuikan River. These specimens come from rocks of comparable age in China. (b) Small shelly fossils of the types found higher in the Kotuikan cliffs; most of the forms seen here are the skeletal spicules of chancellorids, enigmatic baglike animals found widely (and only) in Cambrian rocks. (Images courtesy of Stefan Bengtson)

Figure 1.4. Upstream along the Kotuikan River, showing the angular unconformity between the latest Precambrian-Cambrian succession seen in figure 1.1 and an older package of sedimentary rocks that lies beneath it.

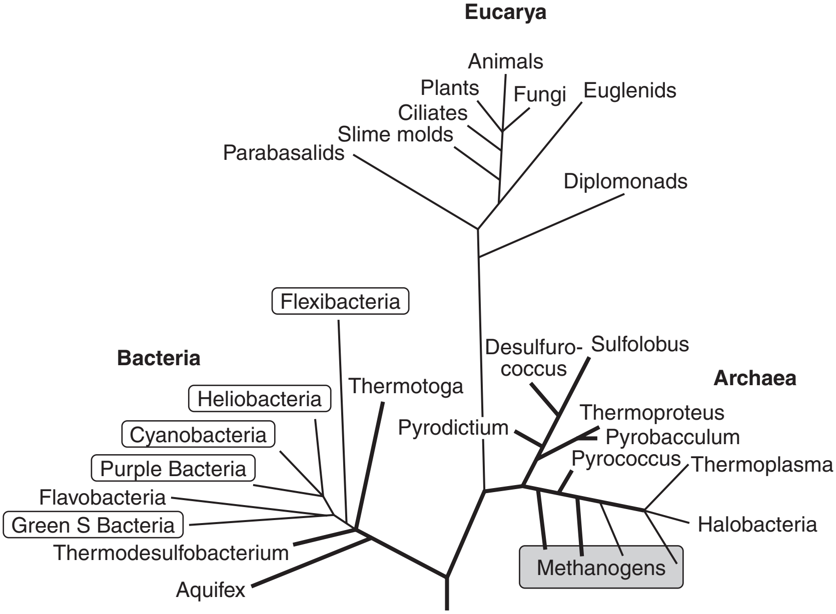

Figure 2.1. The Tree of Life, a depiction of the genealogical relationships of living organisms, based on sequence comparisons of genes that code for RNA in the small subunit of the ribosomes found in all cells. Note the three principal branches, made up of Bacteria, Archaea, and Eucarya. Branch lengths indicate degree of difference among gene sequences; because genes can evolve at different rates, however, this does not necessarily translate into time. Bacterial groups with photosynthetic members are highlighted by clear boxes; methanogenic archeans fall within the shaded box. Heavy lines denote hyperthermophiles—groups of organisms that live at high temperatures. (Adapted from a depiction of the tree by Karl Stetter)

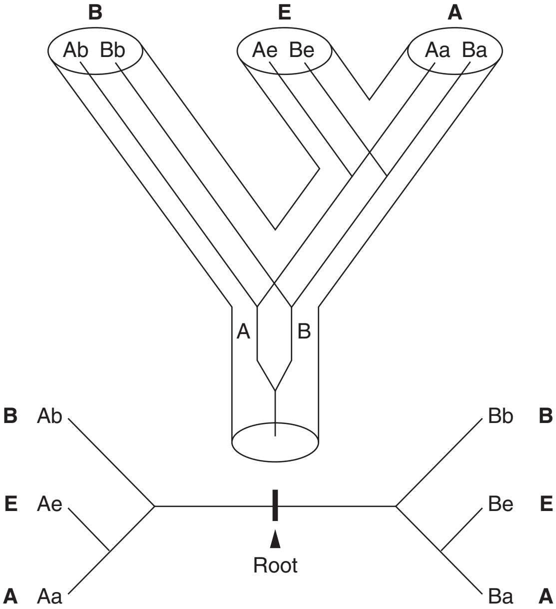

Figure 2.2. Rooting the Tree of Life. *Top:* The genealogical relationships among Bacteria (B), Eucarya (E), and Archaea (A) are shown by the hollow cylindrical branches. Lines within the cylinders show the phylogeny of a gene that duplicated into forms A and B prior to the differentiation of the three domains from their last common ancestor. *Bottom:* The evolutionary relationships among the genes are shown here. Each half tree can be rooted relative to the other, allowing molecular biologists to reconstruct the genealogical relationships among eukaryotes, archaeans, and bacteria.

Figure 3.1. Proterozoic rocks of the Akademikerbreen Group exposed in the glaciated highlands of northeastern Spitsbergen. Each band of light or dark gray rock is about 1,000 feet thick.

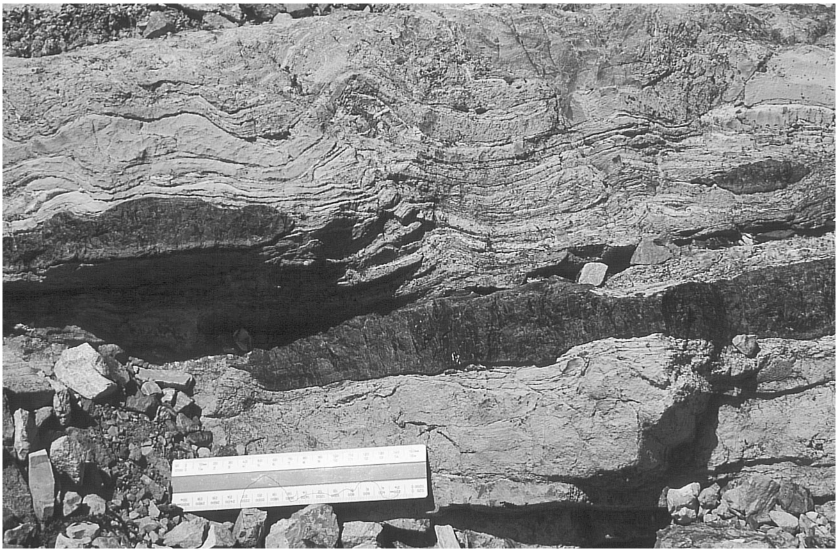

Figure 3.2. Akademikerbreen carbonates deposited near the high-tide mark show wavy laminations characteristic of cyanobacterial mats, as well as tepee structures that provide a key to environmental interpretation. Nodules of black chert within the carbonate beds contain abundant fossils of filamentous microorganisms. Scale is 6 inches long.

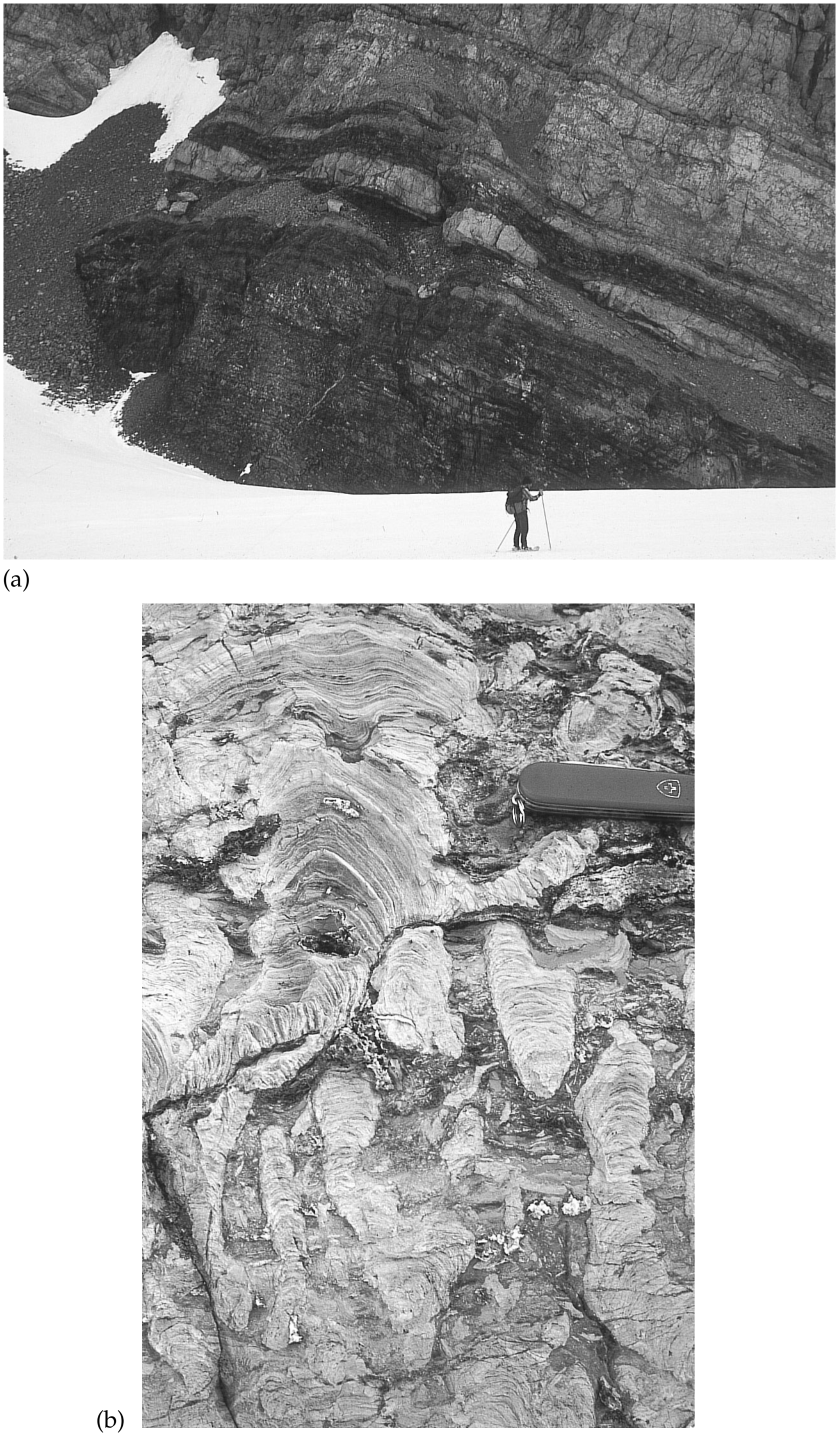

Figure 3.3. Stromatolites in the Akademikerbreen Group. (a) A microbial patch reef, some 15 feet thick, seen in a cliff face. (b) Close-up of a columnar stromatolite, showing the characteristic pattern of convex upward lamination. Note pocketknife for scale.

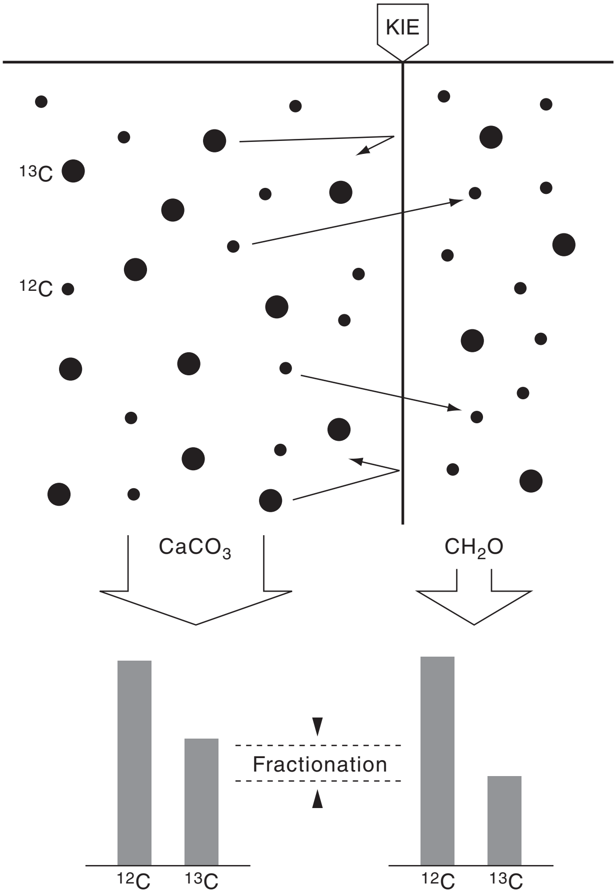

Figure 3.4. Diagram illustrating how photosynthetic organisms fractionate carbon isotopes. Black dots on left side of the diagram depict carbon dioxide molecules that contain ^{12}C (smaller) or ^{13}C (larger). Photosynthetic organisms fix $^{12}CO_2$ preferentially, with the result that the organic matter in photosynthetic organisms (and the organisms that eat them) is depleted in ^{13}C relative to its surroundings; biochemists speak of this as a kinetic isotope effect—hence, the label "KIE" in the figure. The isotopic *fractionation* imparted by organisms will be preserved in sediments as the difference in the ratio of ^{12}C to ^{13}C between limestone and organic matter in the same sample.

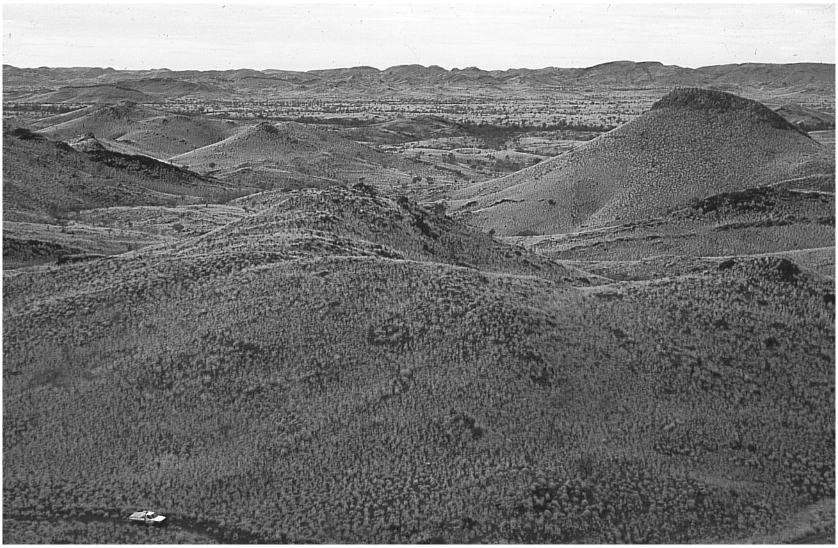

Figure 4.1. These low hills near North Pole, Australia, are built of sedimentary and volcanic rocks formed nearly 3.5 billion years ago. North Pole rocks preserve some of our earliest evidence of life and environments on the young Earth. Note Land Rover for scale.

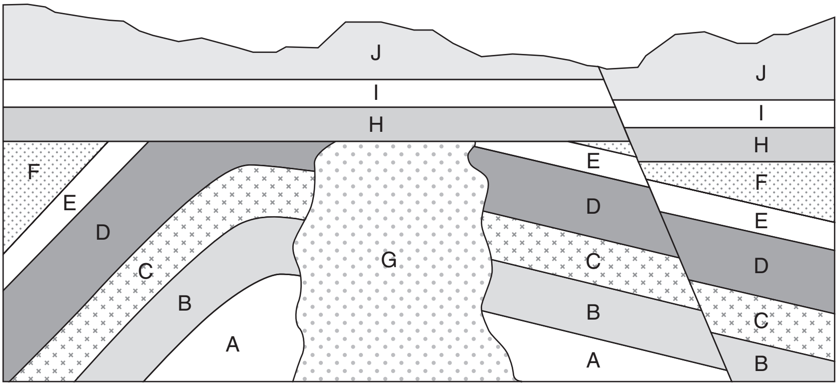

Figure 4.2. A geological cross section, illustrating how geologists sort out rela-tive age relationships.

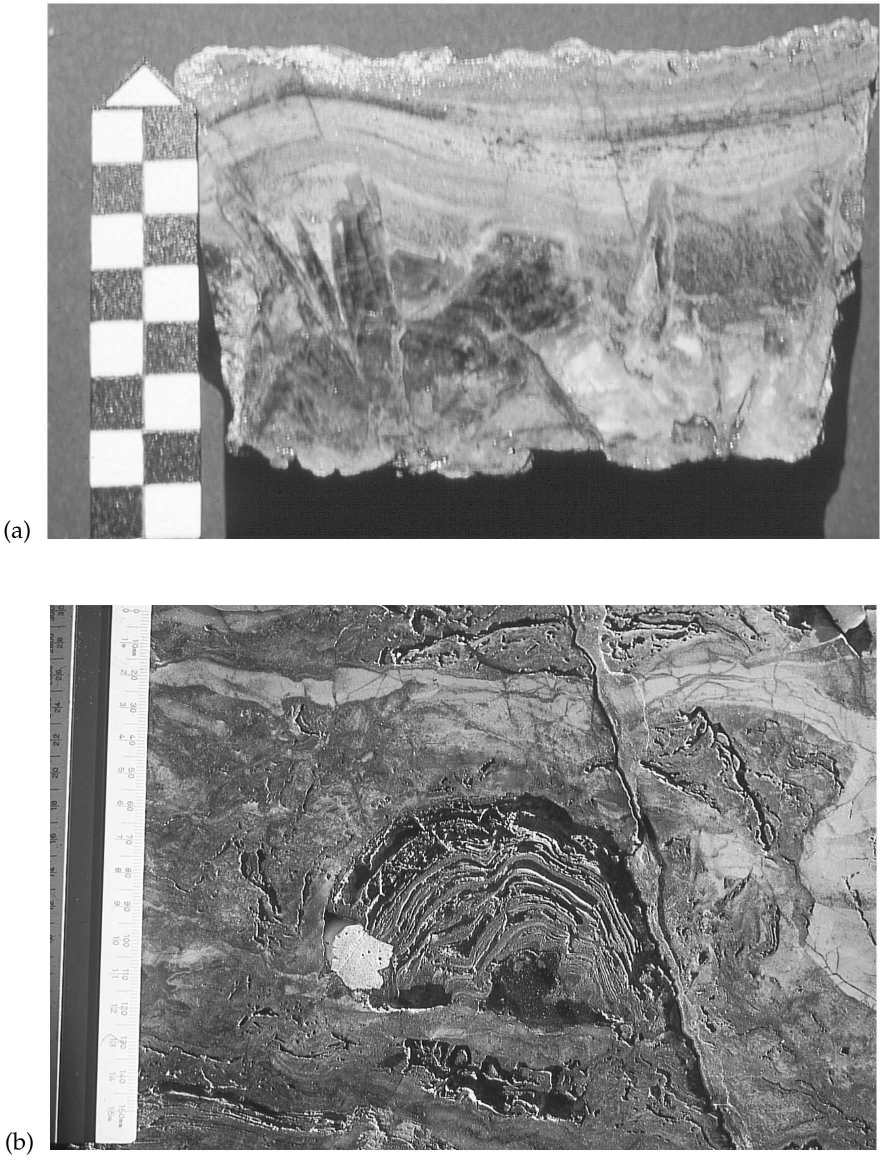

Figure 4.3. Sedimentary features of Warrawoona rocks. (a) Gray-black gypsum crystals (now replaced by silica) that grew on the seafloor and were subsequently buried by thin beds of mud and sand (light layers). Scale bar in centimeters. (b) The stromatolite discovered by Roger Buick and colleagues in the early 1980s, now subject of much debate. Six-inch scale to left. (Photo (a) courtesy of Roger Buick)

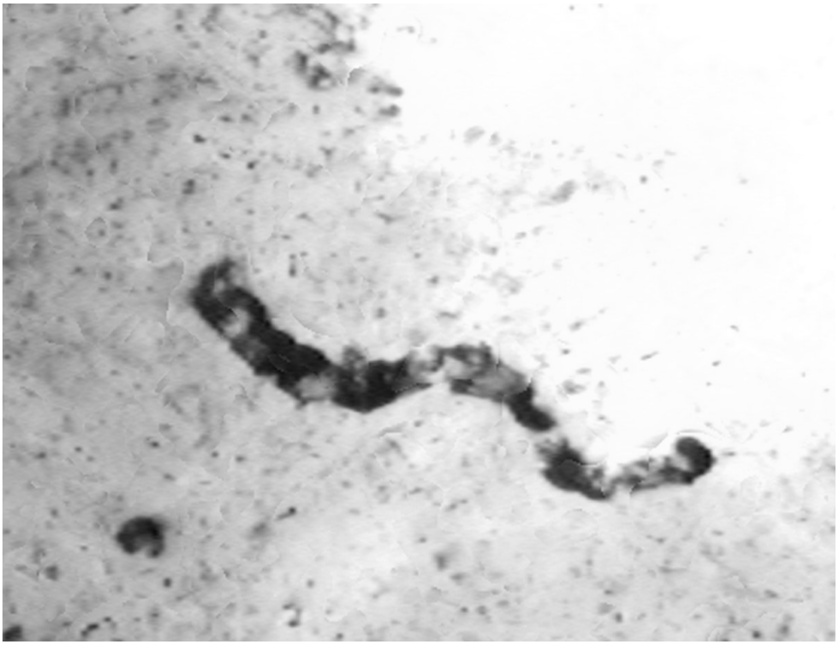

Figure 4.4. Microstructures interpreted as bacterial fossils in Warrawoona chert. The alternative interpretation is that they are simply chains of crystals formed in a hydrothermal vein. (Photo courtesy of Martin Brasier)

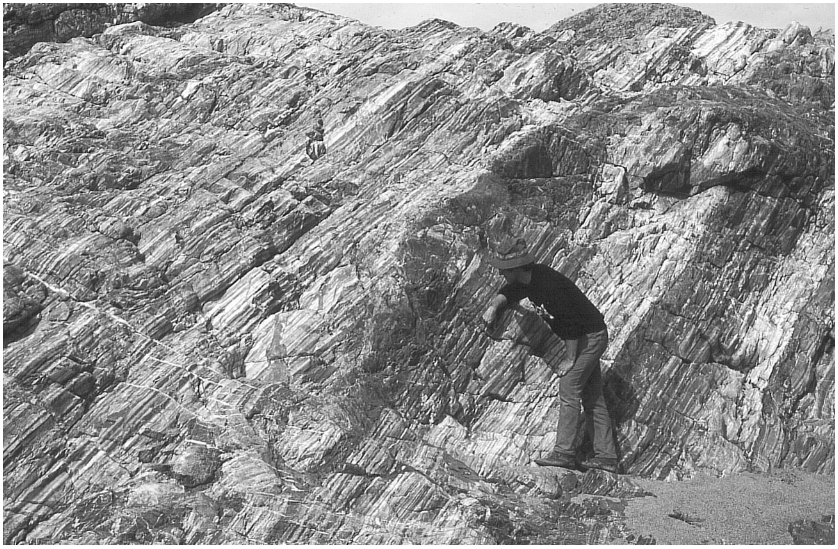

Figure 4.5. Warrawoona chert at Marble Bar, Western Australia. The red (pigmented by iron oxides, gray in picture) and white bands accumulated on the seafloor. In contrast, the black bands cut across other beds and so are younger—and formed in a different way. Warrawoona microstructures interpreted as fossils come from these crosscutting cherts, interpreted as hydrothermal plumbing systems filled by silica.

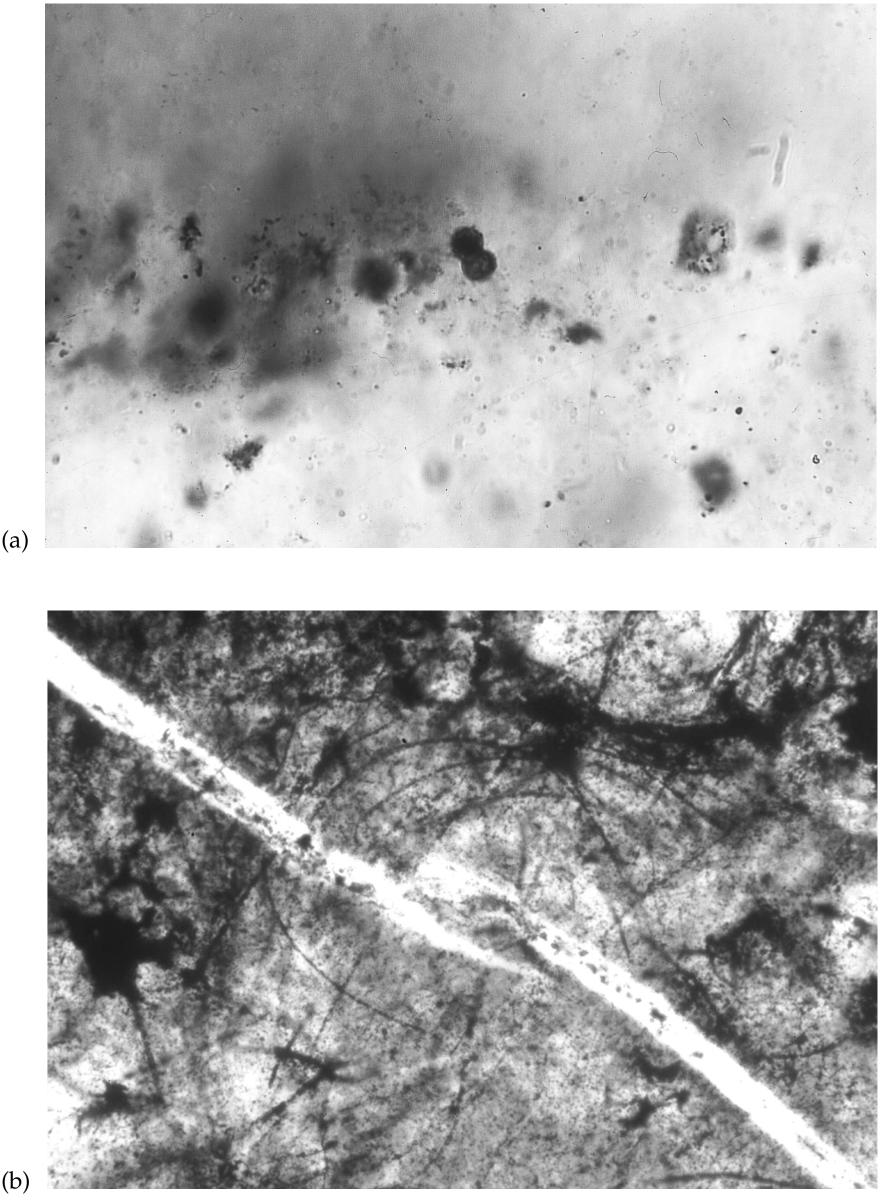

Figure 4.6. (a) Carbonaceous microstructure, possibly preserving a microbe during cell division, in 3.4-billion-year-old rocks from South Africa. Sphere is 4 microns in diameter. (b) Filamentous microfossils in 3.2-billion-year-old rocks from northwestern Australia. Each filament is about 2 microns across. (Photo (b) courtesy of Birger Rasmussen)

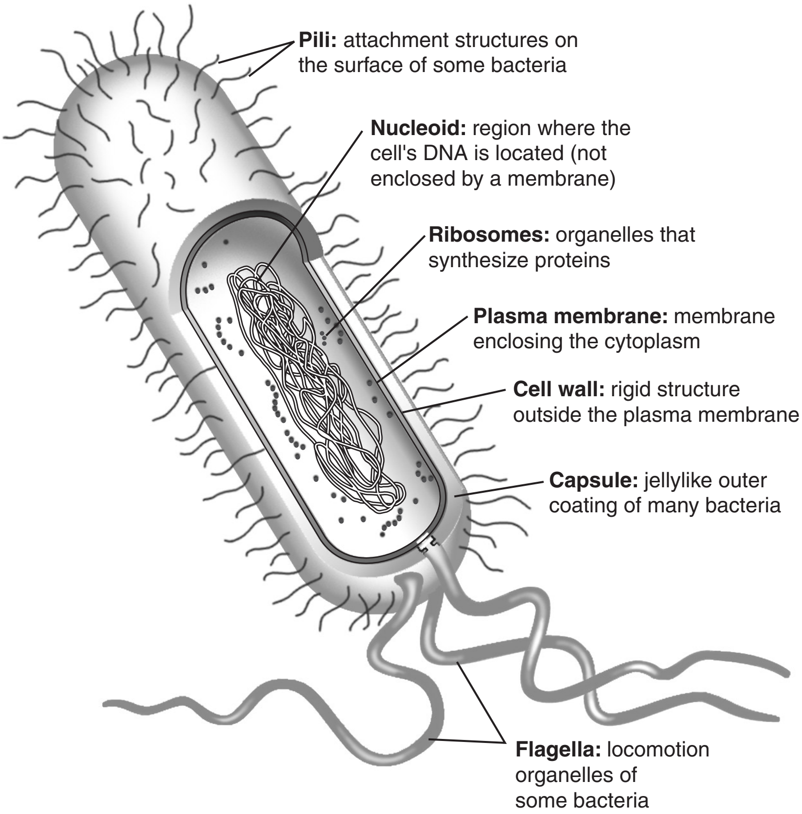

Figure 5.1. The structure and function of a bacterial cell. RNA messages are transcribed from DNA within the nucleoid; these RNA messages are subsequently translated into proteins in chemical factories called ribosomes; cellular metabolism is carried out by pigments and proteins embedded in the cell's membranes. (Reproduced with permission from N. A. Campbell and J. B. Reece, *Biology*, Sixth Edition. Copyright © 2002 by Pearson Education Inc.)

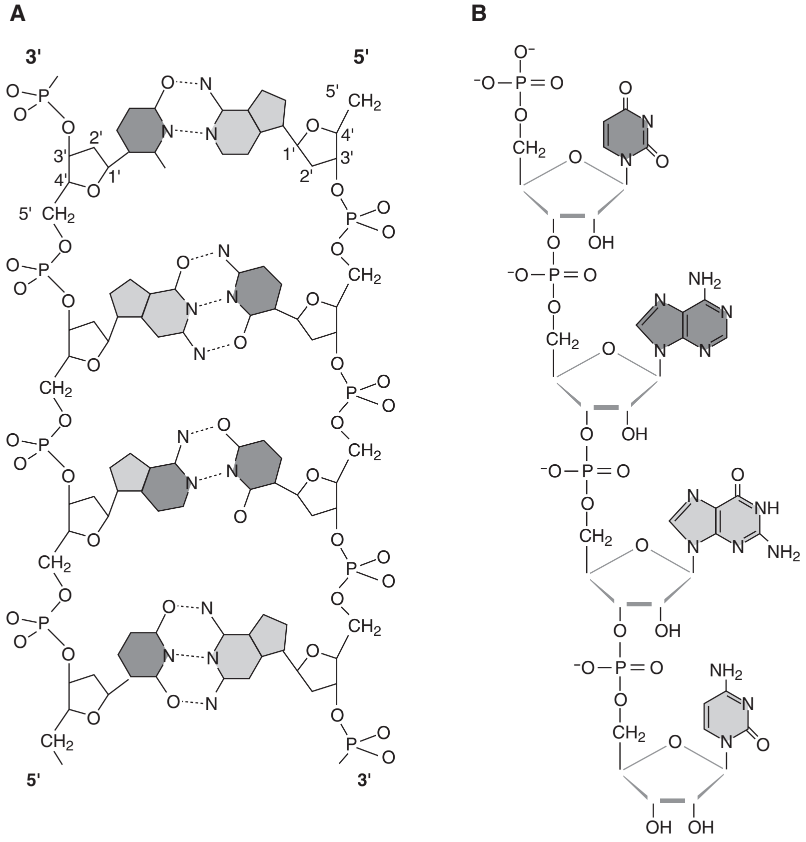

Figure 5.2. The molecular structures of DNA and RNA. (a) DNA, showing how a chemical backbone of phosphate and deoxyribose sugar combines with four bases that provide both molecular information and the bonds that link two strands into a double helix. (b) RNA, built from ribose sugar, phosphate, and four bases (one of which differs from its DNA counterpart). (a) Adapted from illustration by Irving Geis from R. E. Dickerson (1983). The DNA helix and how it is read, *Scientific American* 249: 97–112; rights owned by the Howard Hughes Medical Institute. Not to be reproduced without permission; (b) reproduced with permission from S. Freeman, 2002, *Biological Science*, Prentice Hall)

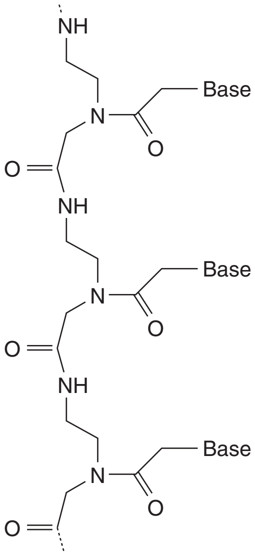

Figure 5.3. The molecular structure of peptide nucleic acid, a nonchiral molecule, illustrating one possible route in the evolution of nucleic acids.

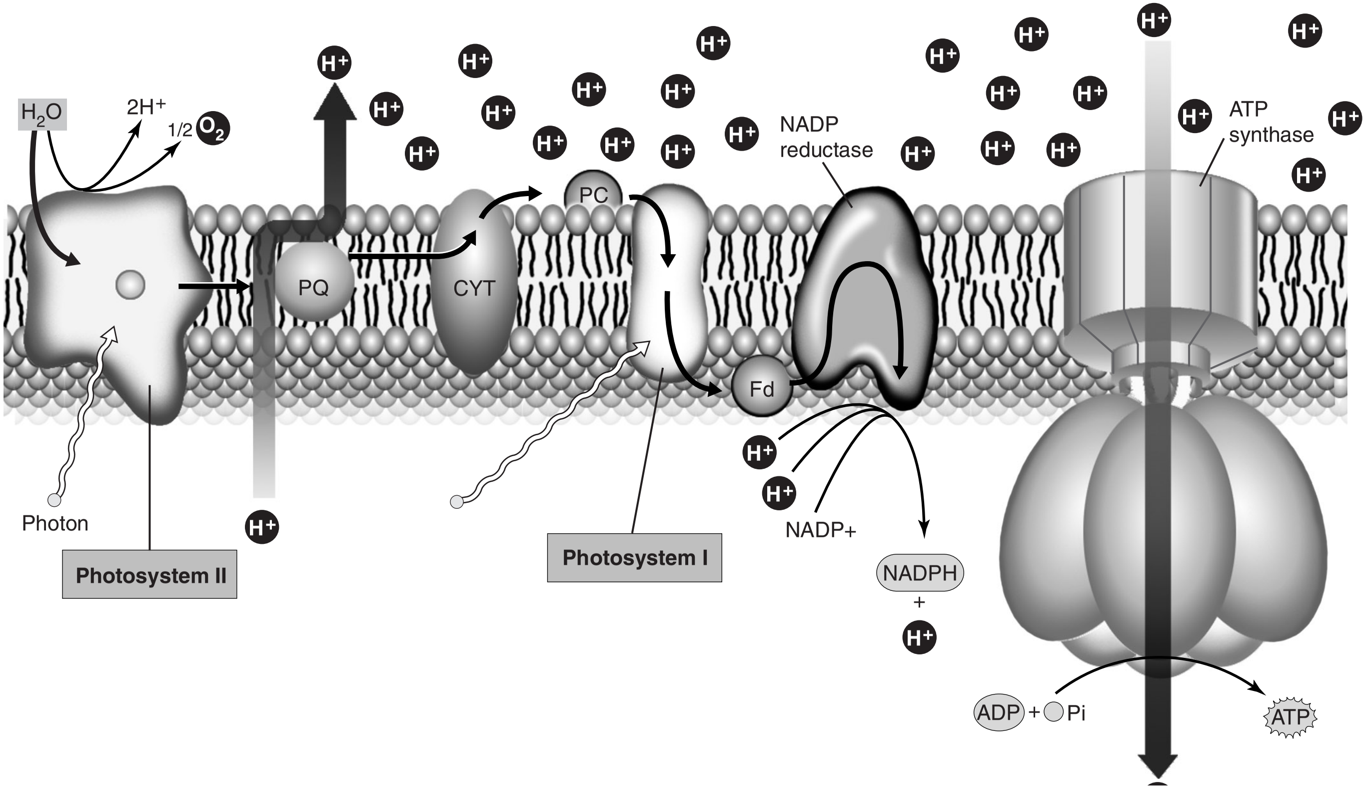
H_2O
$2H^+$
$1/2\ O_2$
Photon
Photosystem II
H^+
PQ
CYT
PC
Photosystem I
Fd
NADP reductase
NADP+
NADPH
+
ATP synthase
ADP
+
Pi
ATP

Figure 5.4. Diagram showing the molecular assembly of photosystems in cyanobacteria and green plants. Chlorophyll and other pigments absorb photons of light and transfer their energy to “excited” electrons. The electrons are then passed in bucket-brigade fashion along a chain of proteins embedded in the photosynthetic membrane. This set of chemical reactions culminates in the formation of ATP and NADPH, molecules that supply the chemical power needed to fix carbon dioxide into sugar (in a separate set of reactions that takes place outside the photosynthetic membrane). Photosynthetic bacteria have one photosystem of linked pigments and proteins. As shown here, cyanobacteria and green plants use two complete photosystems that work together; the chemical breakdown of water in Photosystem II provides the electrons needed for photosynthesis. (Reproduced with permission from W. K. Purves, D. Sadawa, G. H. Orians, and H. C. Heller, 2001. *Life: The Science of Biology*, Sixth Edition, Sinauer Associates and W. H. Freeman and Company)

Figure 6.1. An outcrop of Gunflint chert along the north shore of Lake Superior. The figure in the distance is Elso Barghoorn, the father of Precambrian paleontology.

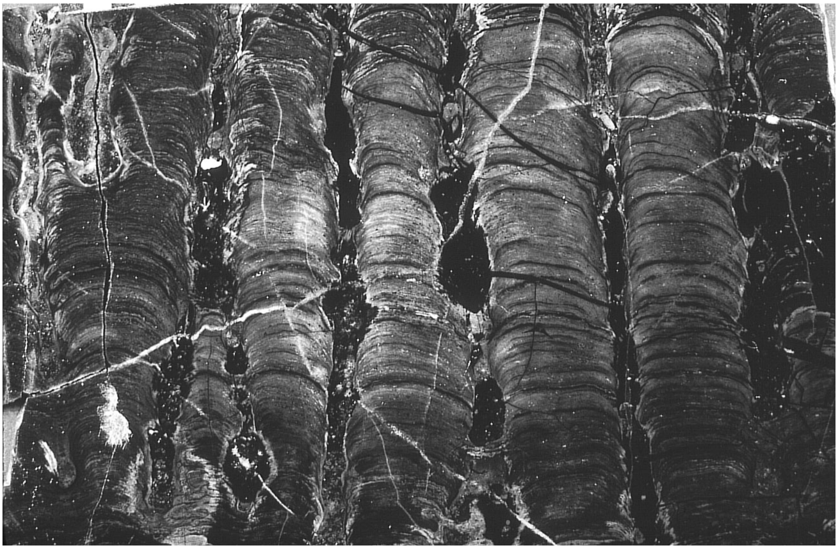

Figure 6.2. Stromatolites in Gunflint chert. Each column is about 1 inch wide.

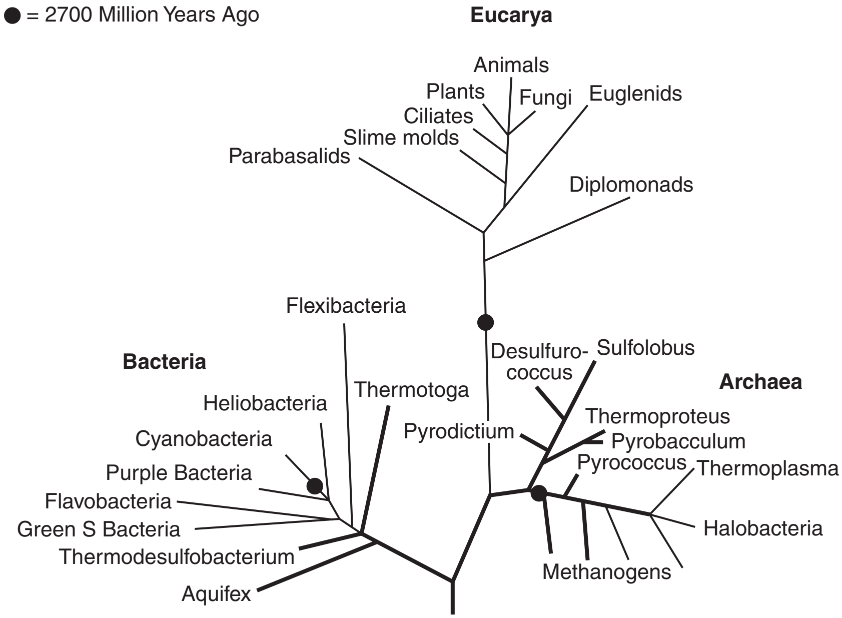

Figure 6.3. Molecular and isotopic biosignatures allow us to place time constraints on branch points in the Tree of Life.

Figure 6.4. A mountain of iron. This landscape in Western Australia is carved out of a massive deposit of 2.5-billion-year-old iron formation.

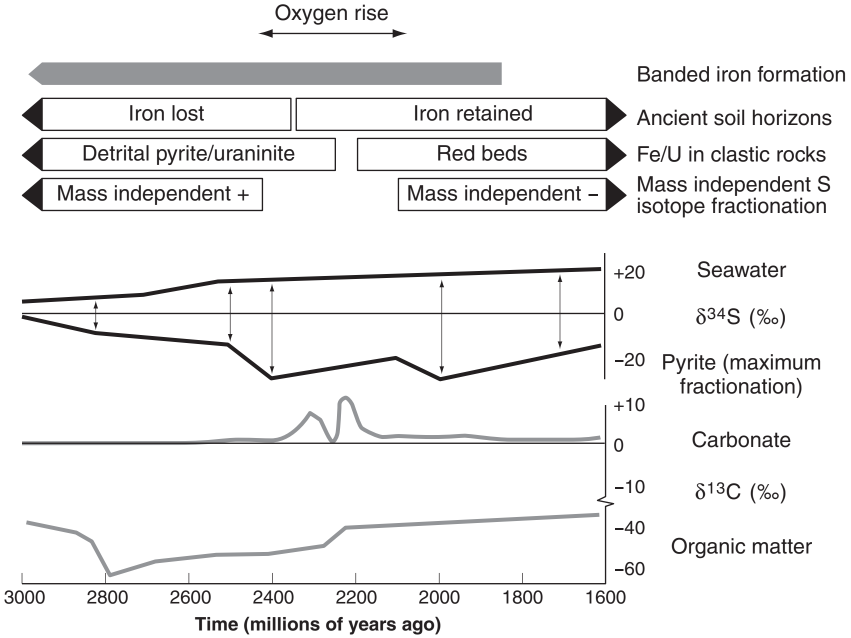

Figure 6.5. Summary of geologic evidence for environmental transition on the early Proterozoic Earth.

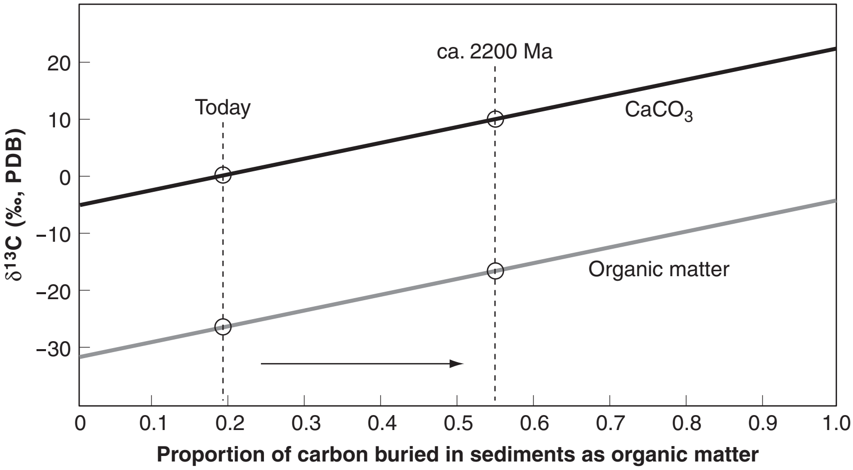

Figure 6.6. The relationship between carbon burial in sediments and the isotopic composition of carbonates and organic matter, after a diagram by John Hayes. Carbon entering the Earth surface system from the mantle (by way of volcanoes) has a δ^{13}C value of about –6‰. (The "delta" notation used by geochemists indicates the difference between ^{13}C/^{12}C in the sample and that of a laboratory standard, expressed in parts per thousand—symbolized by ‰.) If all carbon entering the system were deposited as carbonate, the δ^{13}C value of that carbonate would also be –6‰, because, in terms of isotopes, what comes out must equal what went in. For the same reason, if all carbon were buried as organic matter, *its* δ^{13}C value would be –6‰. In the real world, where carbon enters sediments as a mixture of carbonate and organic matter, the total isotopic composition of carbon leaving the system must still match that coming in; this is achieved when isotopic compositions for carbonate and organic matter follow the diagonal trend lines shown in the graph. Today, for example, carbon burial in sediments is about 81% carbonate and 19% organic matter, and δ^{13}C values of carbonate and organic matter are about 0‰ and –28‰, respectively. In 2.2-billion-year-old rocks, however, carbonate δ^{13}C values are commonly about +8‰, whereas the δ^{13}C values of organic matter hover around –20‰, suggesting that during this interval, rates of organic carbon burial matched those of carbonate deposition.

Figure 7.1. The Great Wall along the Kotuikan River in northern Siberia. The wall is built of flat-lying carbonate rocks deposited along the edge of the ocean some 1.5 billion years ago.

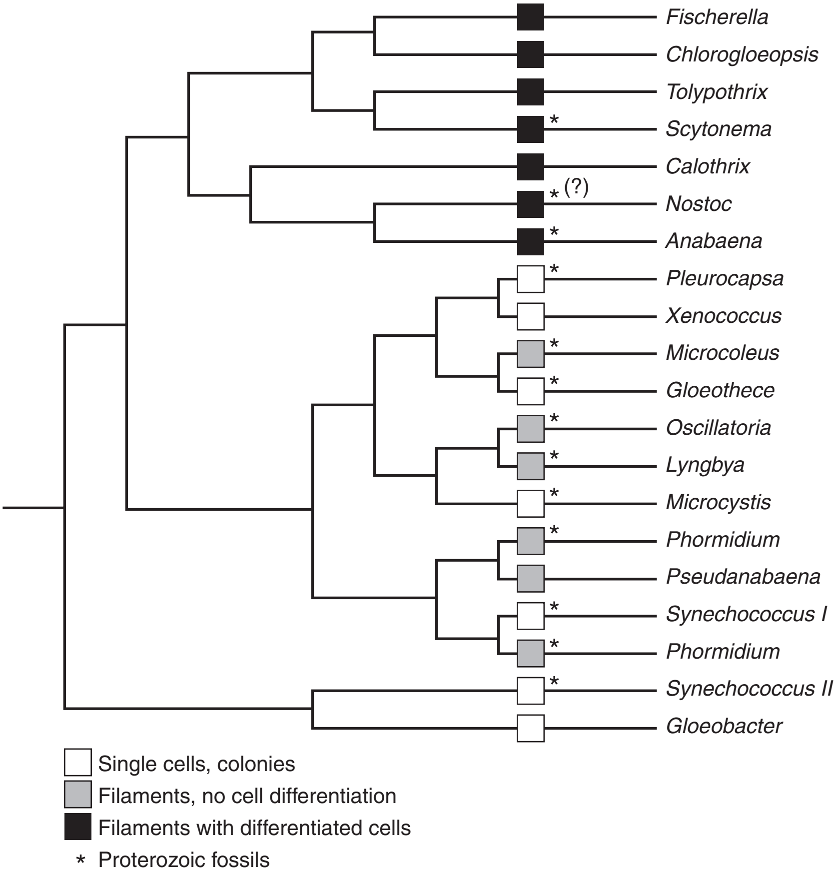

Figure 7.2. A tree showing evolutionary relationships among living cyanobacteria. Note that cyanobacteria with specialized cells fall on a fairly late branch of the tree. This means that fossils showing cell differentiation can place an upper bound on when the tree's major branches formed. (Phylogenetic data courtesy of Akiko Tomitani)

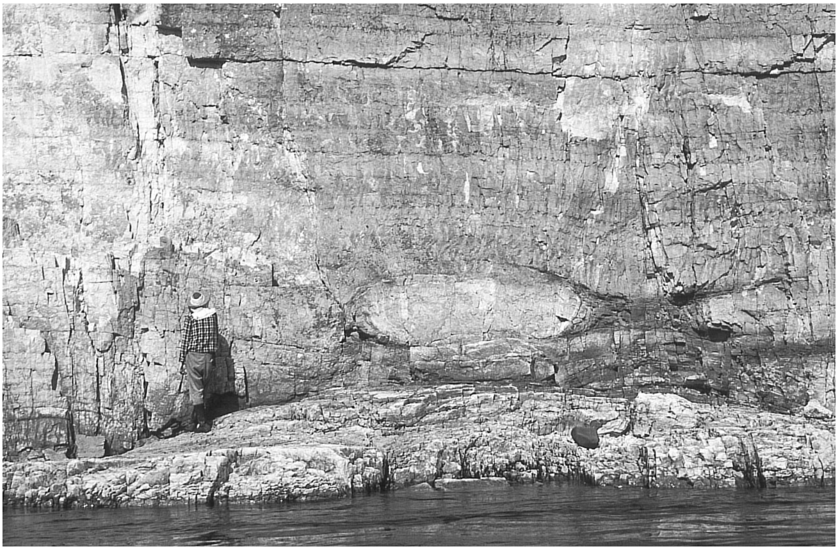

Figure 7.3. Stromatolitic reefs in the 1.5-billion-year-old Bil'yakh Group, northern Siberia. The bunlike feature to the right of Misha Semikhatov (who, for scale, is precisely 2 meters tall when wearing a hat) is a small reef. Misha is standing on the curved upper surface of a second, larger reef. And the wall extending above him is part of still another reef, this one the size of a small office building.

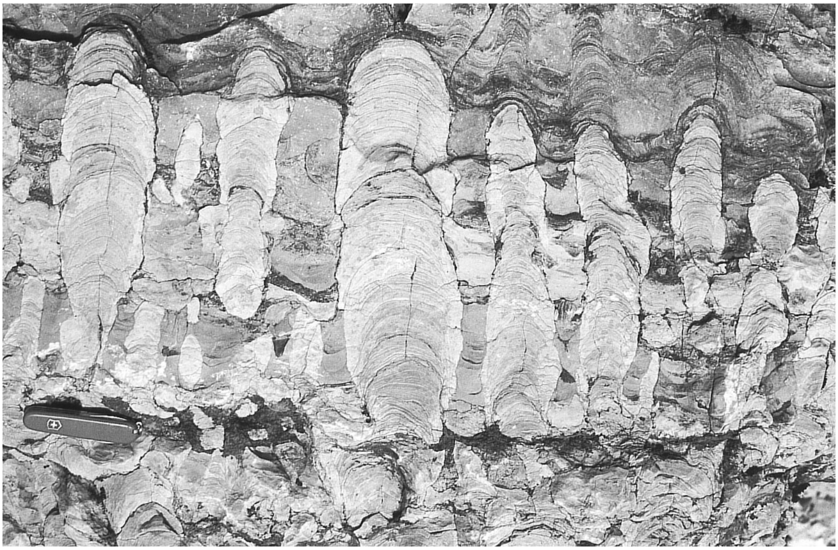

Figure 7.4. Stromatolites in mid-Proterozoic carbonate rocks from Siberia. The largest column is about 4 inches wide.

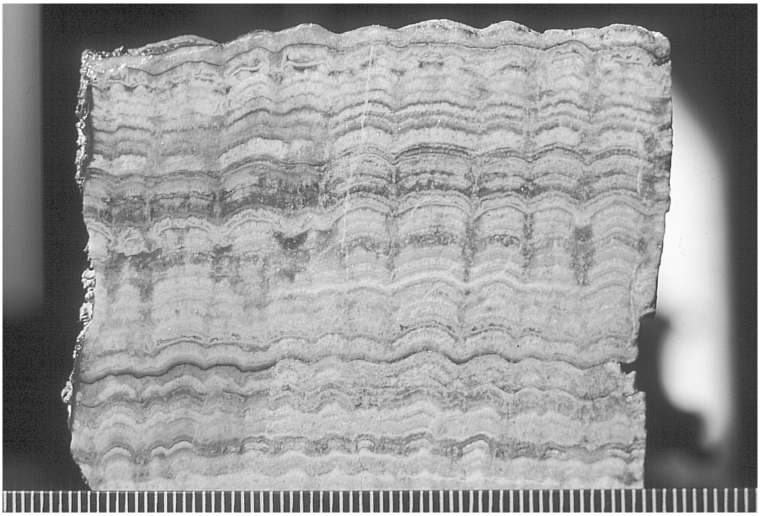

Figure 7.5. Fingerlike laminated structures, each 0.4 inches across, formed by calcium carbonate precipitation without any obvious participation by microbial mats. This specimen, collected by Linda Kah, comes from a 1.2-billion-year-old tidal-flat deposit on Baffin Island, northern Canada.

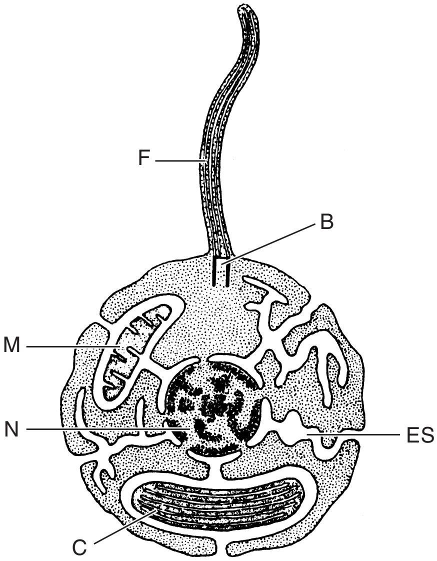

Figure 8.1. The internal organization of the eukaryotic cell. Note that the membranes of eukaryotes, including the endomembrane system (ES), define a space that contains the nucleus (N) and cytoplasm. Chloroplasts (C) and mitochondria (M), however, lie outside this space. Diagram also shows uniquely eukaryotic flagellum (F) anchored by a basal body (B). (Adapted from a figure by Max Taylor)

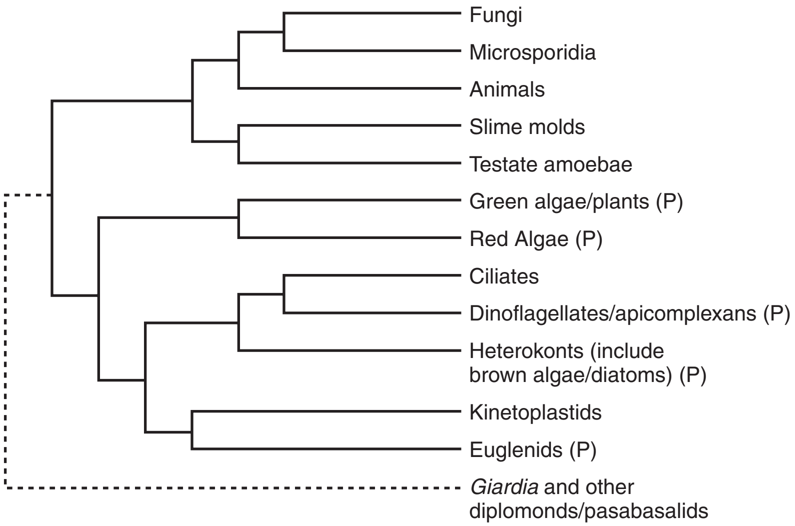

Figure 8.2. A current hypothesis of genealogical relationships among eukaryotic organisms, based on molecular sequence comparisons of ten genes. Note the dotted line that connects diplomonads (which include *Giardia lamblia*) and parabasalids to the remainder of tree. This indicates the uncertainty surrounding the nature and composition of early branches on the tree. Groups with photosynthetic members marked by P. (Redrawn from a figure by Sandra Baldauf)

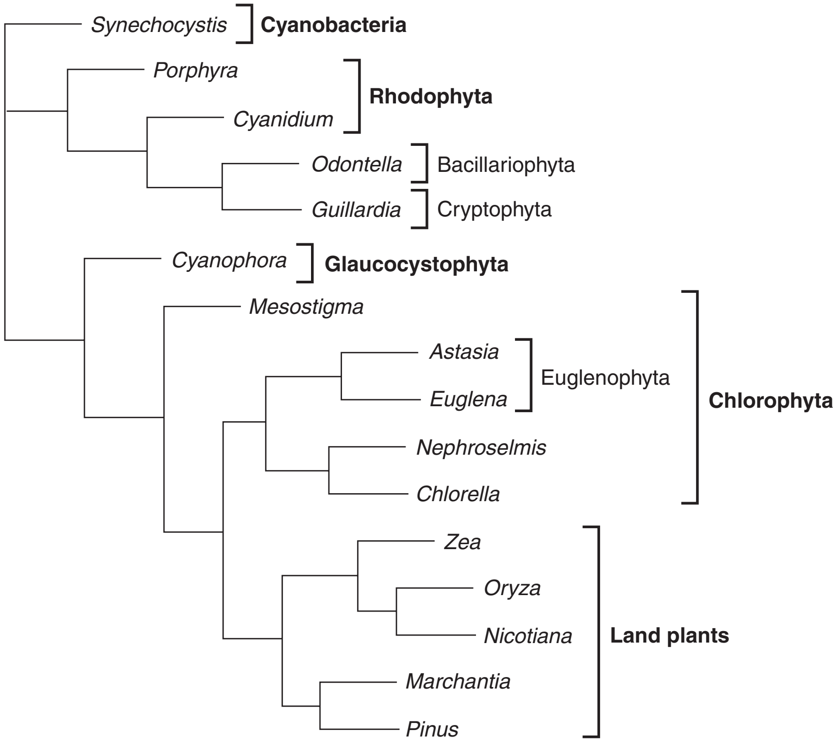

Figure 8.3. Genealogical relationships among chloroplasts, based on molecular sequence comparisons. Note that the chloroplast tree does not show the same relationships as trees based on nuclear gene sequences. This strongly supports the idea that many eukaryotes acquired photosynthesis by engulfing other eukaryotic cells. Photosynthetic euglenids, for example, appear to be derived from endosymbiotic green algae, while the chloroplasts in cryptophyte and heterokont algae (here represented by the Bacillariophyta, or diatoms) seem to be descended from red algal symbionts. (Phylogenetic data courtesy of Paul Falkowski)

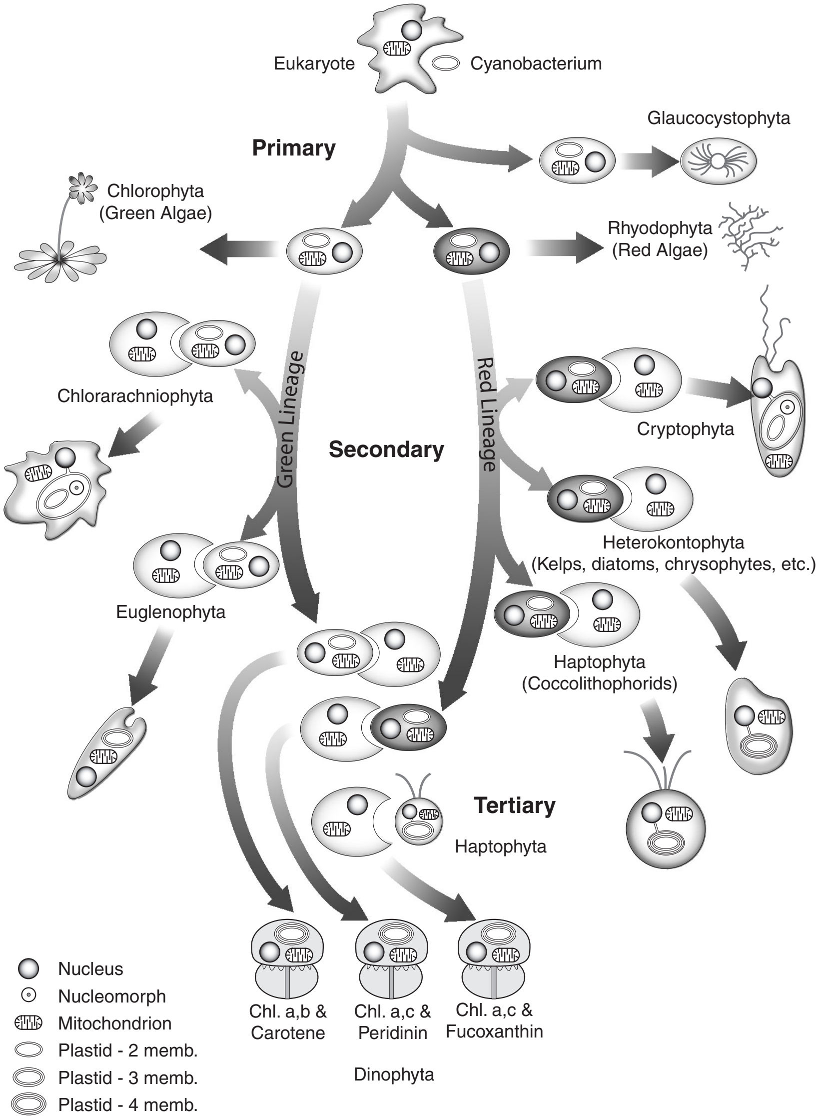

Figure 8.4. A summary of the endosymbiotic events by which photosynthesis spread through the Eucarya. (Reproduced with permission from an illustration by Charles Delwiche)

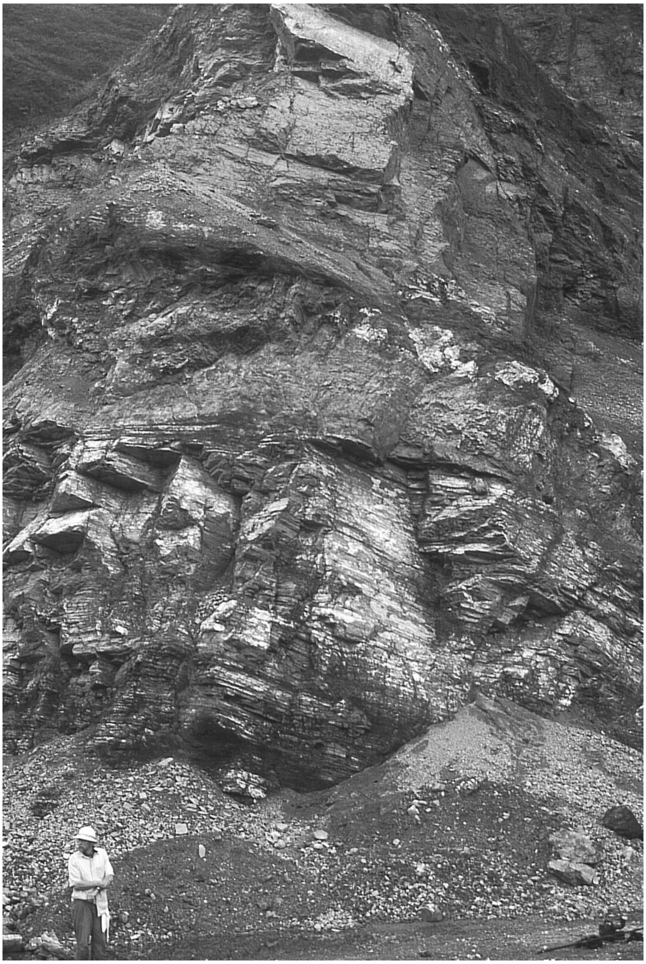

Figure 9.1. Fossiliferous phosphate rocks of the Doushantuo Formation, exposed in a quarry at Weng'an, China.

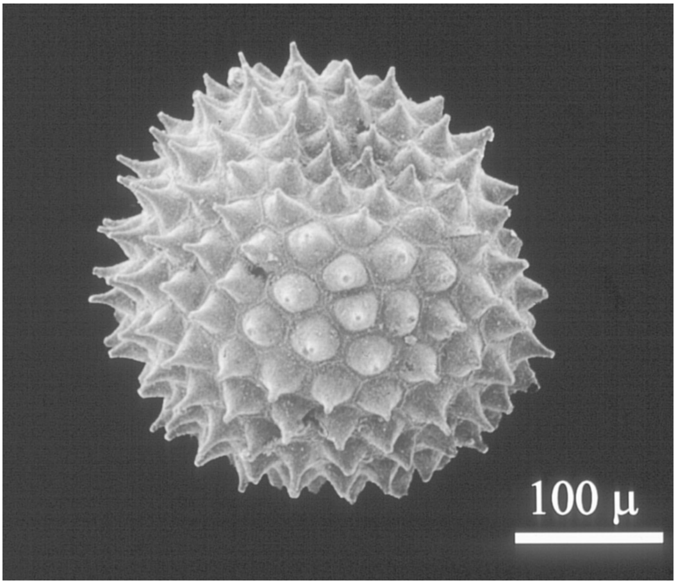

Figure 9.2. A spiny microfossil found commonly in Doushantuo cherts and phosphatic rocks. Such fossils are thought to be the reproductive spores of eukaryotic organisms. Fossil is 250 microns in diameter. (Image courtesy of Shuhai Xiao)

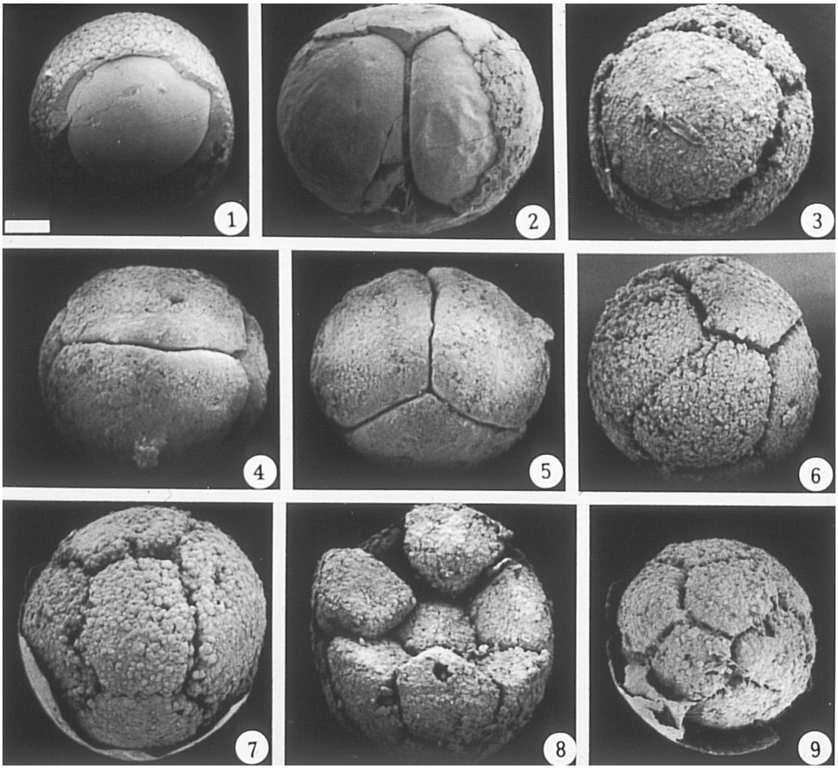

Figure 9.3. Eggs and embryos of early animals, preserved in Doushantuo phosphate. Each fossil is 400–500 microns in diameter. (Images courtesy of Shuhai Xiao)

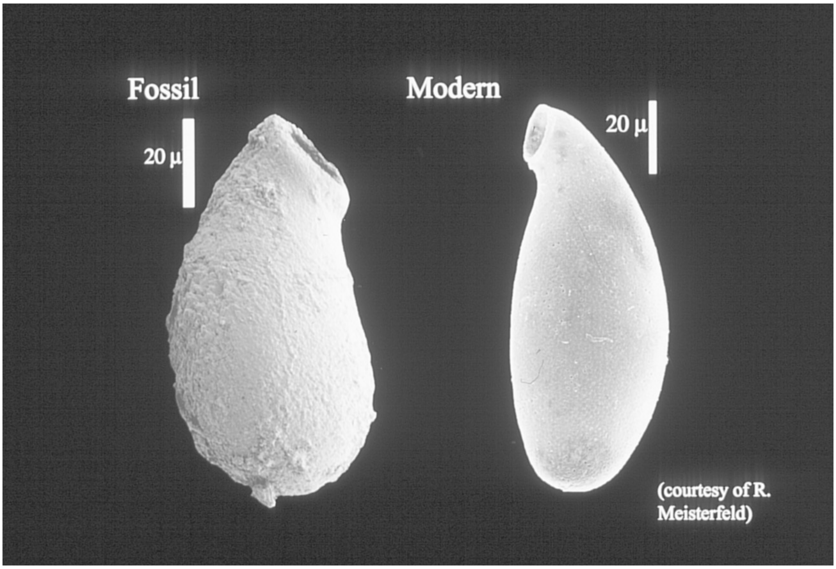

Figure 9.4. Vase-shaped fossil from ca. 750-million-year-old rocks of the Grand Canyon compared with a modern testate amoeba. Note scale on photo. (Figure courtesy of Susannah Porter)

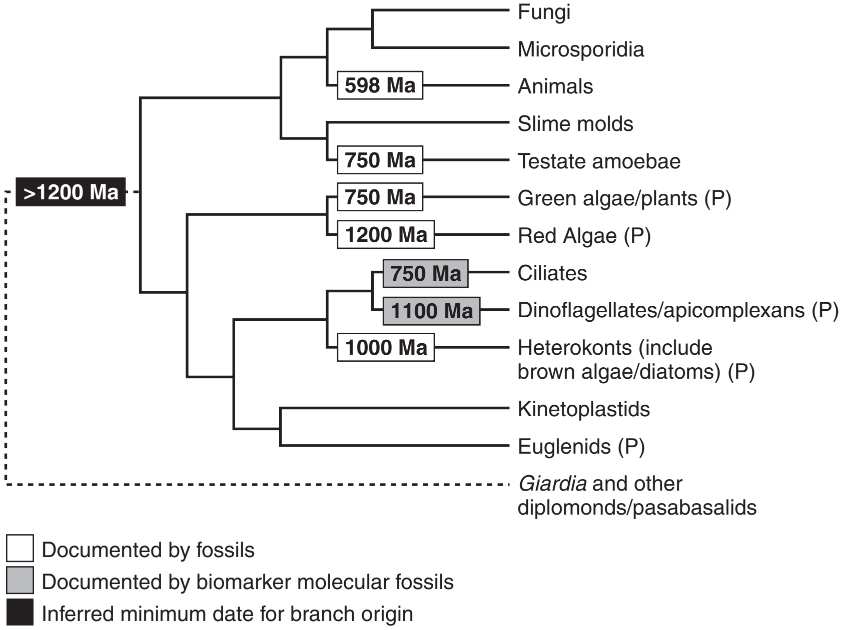

Figure 9.5. The eukaryotic phylogeny first shown in figure 8.2, here trimmed with the dates of early eukaryotic fossils.

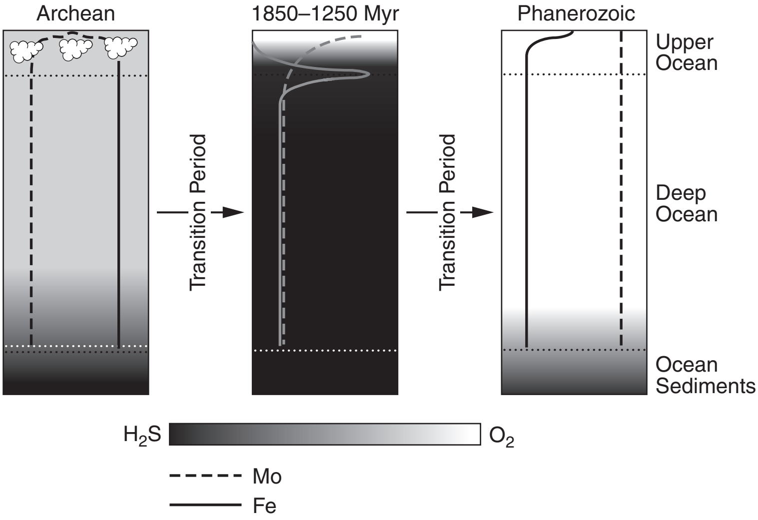

Figure 9.6. Triptych illustrating the three phases of ocean evolution. Early oceans contained little oxygen, but relatively abundant iron. Modern oceans contain abundant oxygen and little iron. In between, during a long-lived state that may have lasted from 1.8 billion years ago until near the end of the Proterozoic Eon, the oceans are thought to have had moderate oxygen in surface waters, but hydrogen sulfide at depth. In such an ocean, biologically important trace elements such as iron and molybdenum (concentrations, higher to the right, illustrated by vertical lines) may have been in seriously short supply. (Reprinted with permission from A. D. Anbar and A. H. Knoll, 2002. Proterozoic ocean chemistry and evolution: a bioinorganic bridge? *Science* 297: 1137–1142. Copyright 2002 American Association for the Advancement of Science)

Figure 10.1. Sedimentary rocks of the Nama Group rise out of the Namibian desert. The large gray mounds to the left of the mesa and near its top are microbial reefs that contain calcified animal fossils. Ediacaran impressions occur in sandstones that form the conspicuous ledge high on the hill.

Figure 10.2. Simple track fossils made by bilaterian animals in a latest Proterozoic seaway. The specimen comes from South Australia. Each trail is a bit over 1 millimeter wide.

Figure 10.3. *Parvancorina*, a problematic fossil that superficially (and, I think, only superficially) resembles trilobites.

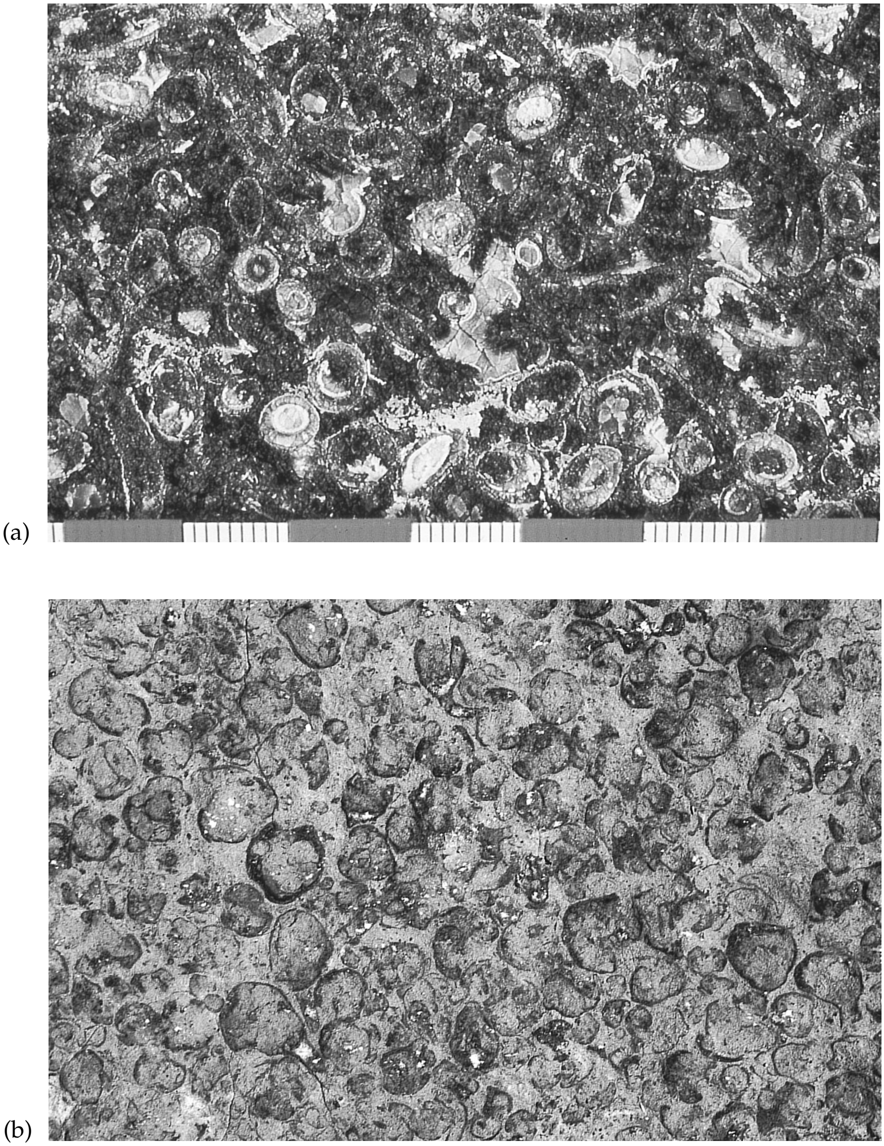

Figure 10.4. Calcified fossils from microbial reefs of the Nama Group. (a) *Cloudina*, tubular fossils lightly mineralized by calcium carbonate. (b) *Namacalathus* population showing the variety of shapes seen on rock surfaces in Nama limestones. Note centimeter scale bar in upper photo.

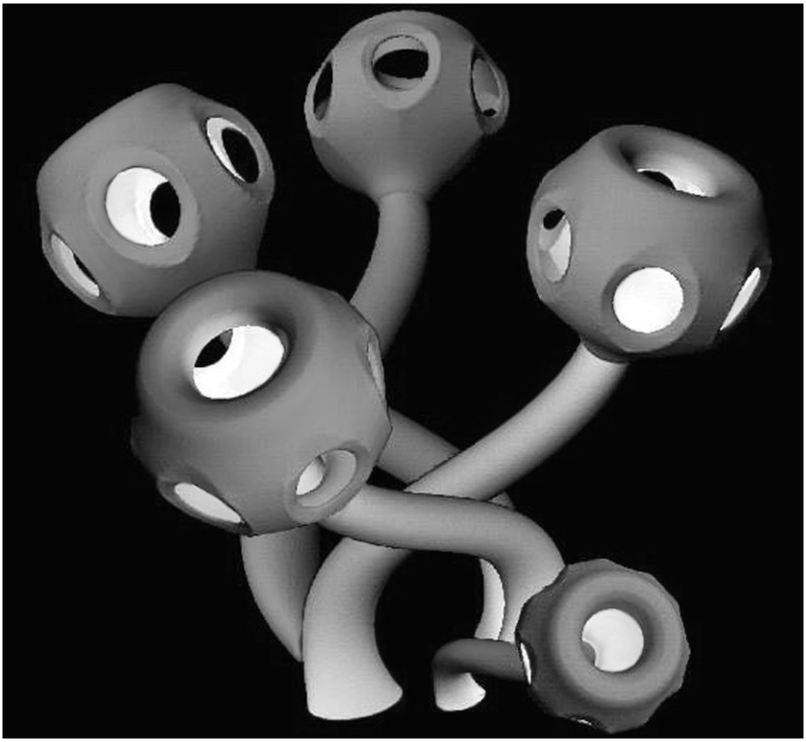

Figure 10.5. Virtual fossils of *Namacalathus*, reconstructed from digitized images. (Image generated by Wes Watters)

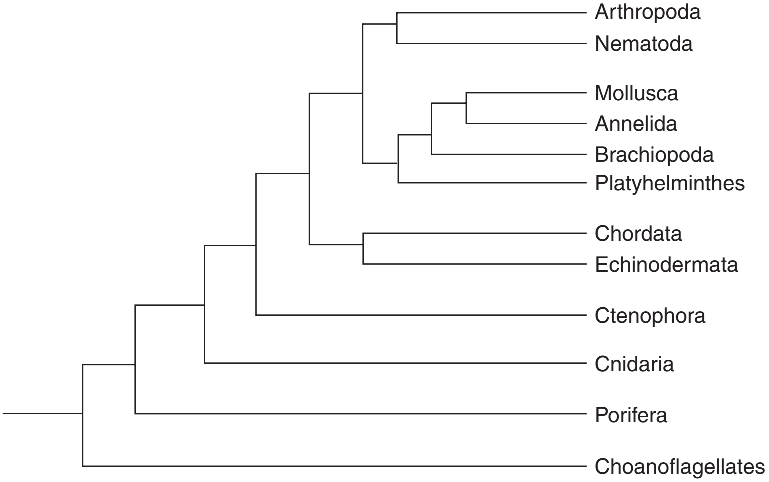

Figure 11.1. Evolutionary relationships among animal phyla, as indicated by molecular phylogeny.

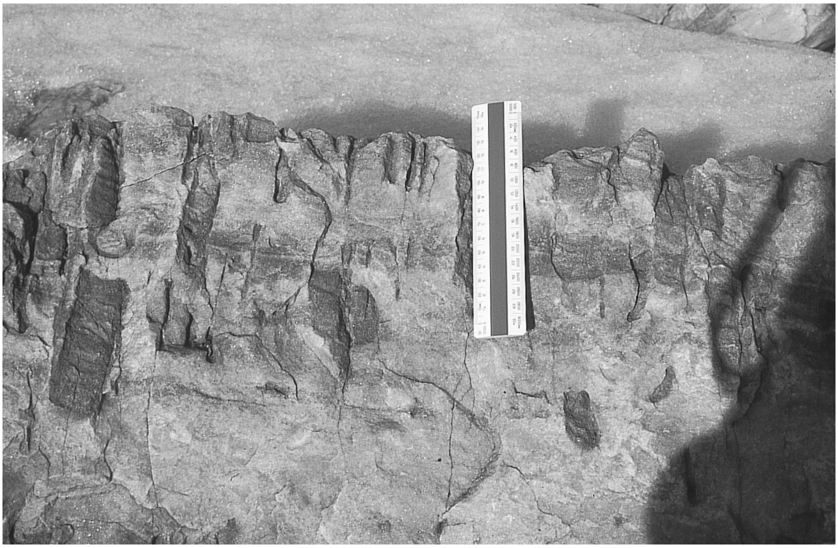

Figure 11.2. U-shaped burrows made by invertebrates in Cambrian beach sands. Polychaete worms make similar burrows today.

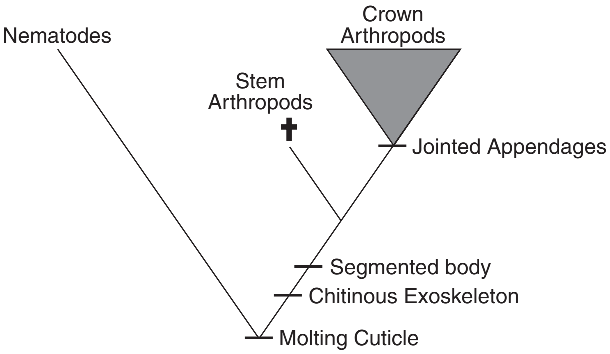

Figure 11.3. Diagram illustrating the concepts of stem and crown groups, as exemplified by arthropod evolution.

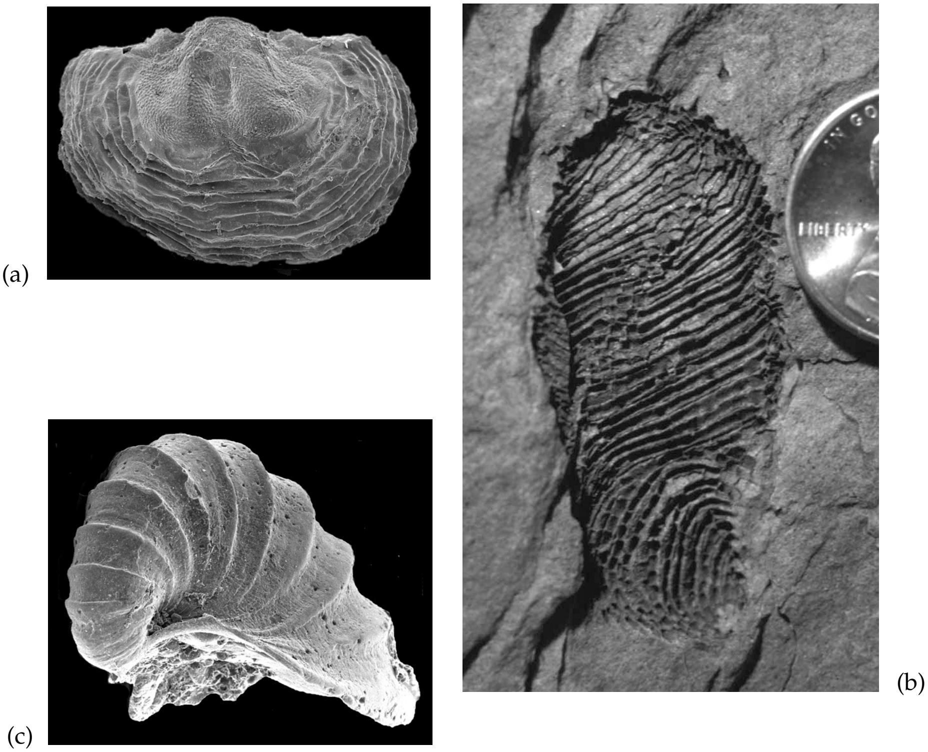

Figure 11.4. Cambrian fossils interpreted as stem groups of bilaterian phyla or classes. (a) an Early Cambrian brachiopod. (b) A helicoplacoid echinoderm. (c) A spirally coiled mollusk from basal Cambrian rocks. (Image (a) courtesy of Leonid Popov; (b) courtesy of David Bottjer and Stephen Dornbos; (c) courtesy of Stefan Bengtson)

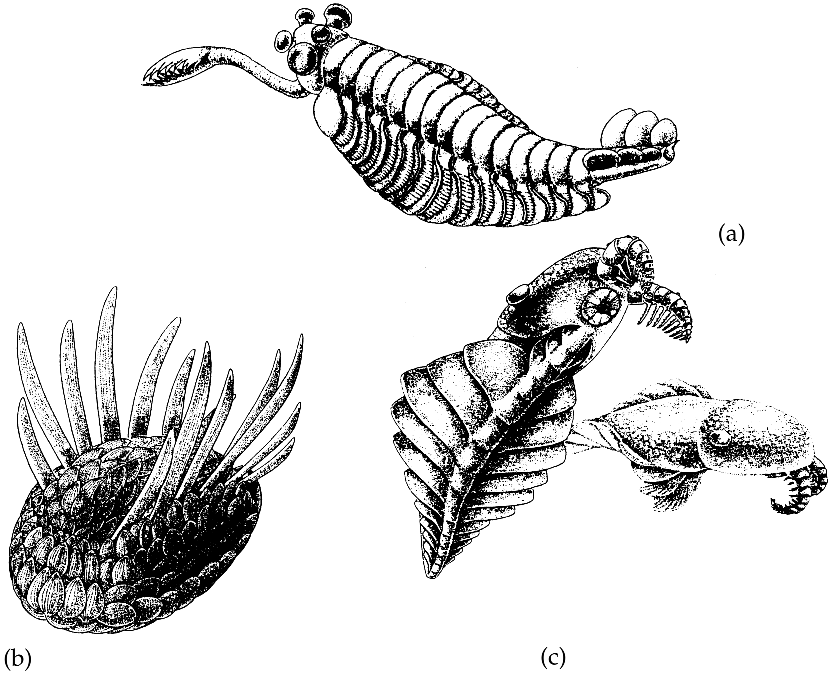

Figure 11.5. "Weird wonders" from the Middle Cambrian Burgess Shale. (a) *Opabinia*. (b) *Wiwaxia*. (c) *Anomalocaris*. (From S. J. Gould's *Wonderful Life,* W. W. Norton and Company, Inc., reproduced with permission)

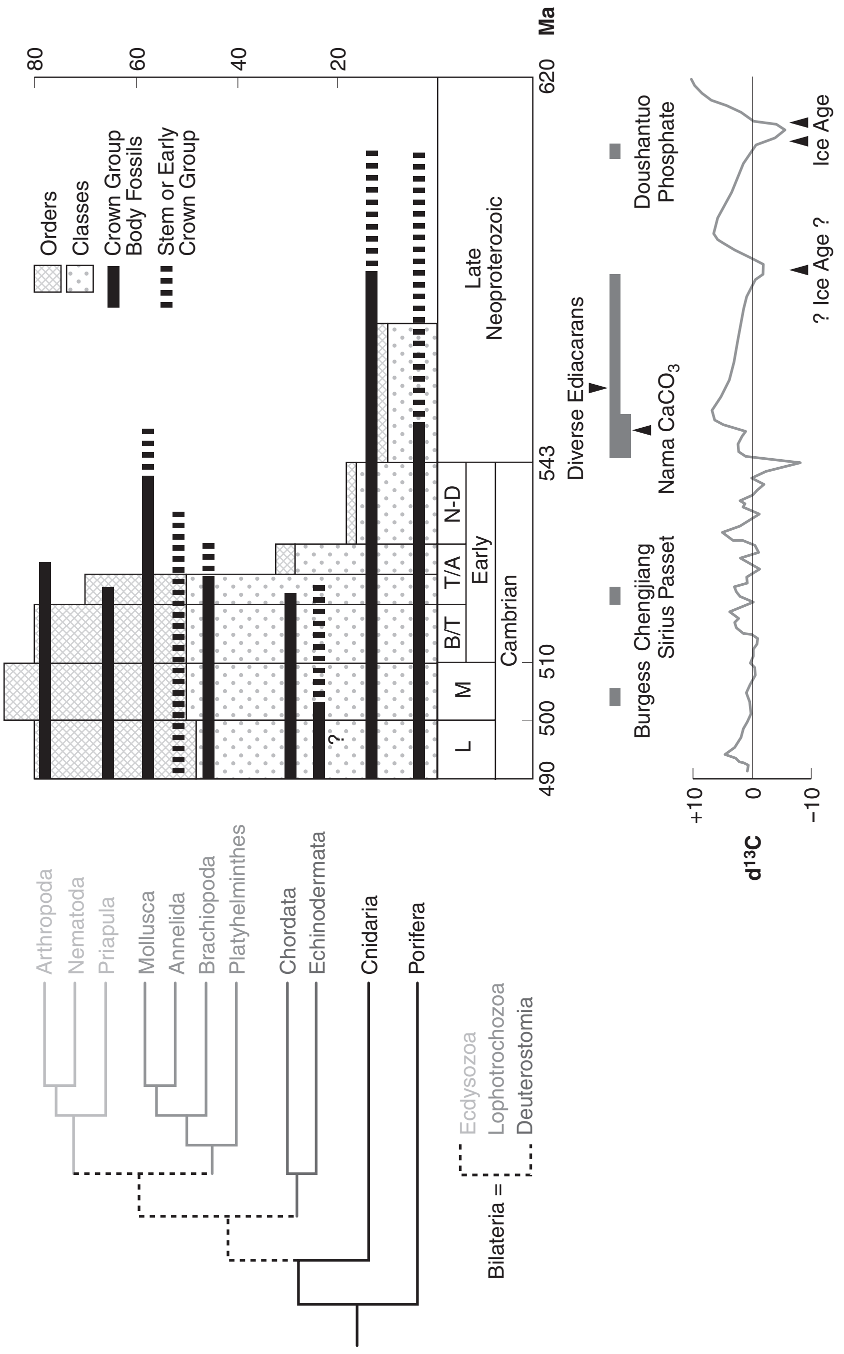
Arthropoda
Nematoda
Priapula
Mollusca
Annelida
Brachiopoda
Platyhelminthes
Chordata
Echinodermata
Cnidaria
Porifera
Bilateria =
Ecdysozoa
Lophotrochozoa
Deuterostomia
Orders
Classes
Crown Group Body Fossils
Stem or Early Crown Group
80
60
40
20
Ma
490
500
510
543
620
L
M
B/T
T/A
N-D
Early
Cambrian
Late Neoproterozoic
?
Diverse Ediacarans
Nama $CaCO_3$
Burgess
Chengjiang
Sirius Passet
Doushantuo Phosphate
? Ice Age ?
Ice Age
d¹³C
+10
0
−10

Figure 11.6. A summary of animal phylogeny and Cambrian evolution, showing first-known appearances of stem and crown group members of extant phyla, as well as animal diversity through the Cambrian Period. To aid discussion in chapter 12, the record of carbon isotopes across the Proterozoic-Cambrian boundary is also shown. (Reprinted with permission from A. H. Knoll and S. B. Carroll, 1999. Early animal evolution: emerging views from comparative biology and geology. *Science* 284: 2129–2137. Copyright 1999 American Association for the Advancement of Science)

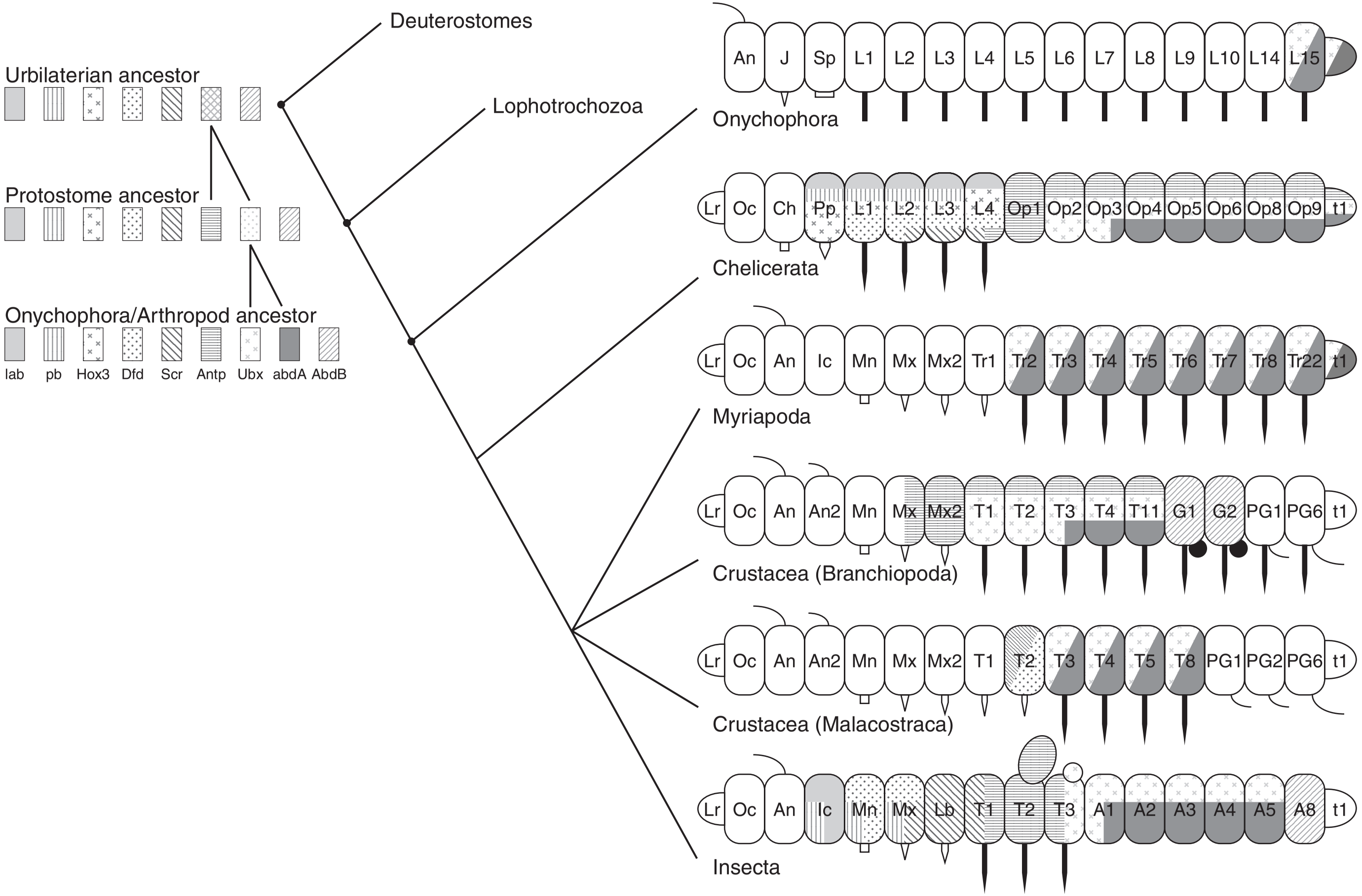
Urbilaterian ancestor
Protostome ancestor
Onychophora/Arthropod ancestor
lab
pb
Hox3
Dfd
Scr
Antp
Ubx
abdA
AbdB
Deuterostomes
Lophotrochozoa
Onychophora
An J Sp L1 L2 L3 L4 L5 L6 L7 L8 L9 L10 L14 L15
Chelicerata
Lr Oc Ch Pp L1 L2 L3 L4 Op1 Op2 Op3 Op4 Op5 Op6 Op8 Op9 t1
Myriapoda
Lr Oc An Ic Mn Mx Mx2 Tr1 Tr2 Tr3 Tr4 Tr5 Tr6 Tr7 Tr8 Tr22 t1
Crustacea (Branchiopoda)
Lr Oc An An2 Mn Mx Mx2 T1 T2 T3 T4 T11 G1 G2 PG1 PG6 t1
Crustacea (Malacostraca)
Lr Oc An An2 Mn Mx Mx2 T1 T2 T3 T4 T5 T8 PG1 PG2 PG6 t1
Insecta
Lr Oc An Ic Mn Mx Lb T1 T2 T3 A1 A2 A3 A4 A5 A8 t1

Figure 11.7. Expression of *Hox* genes along the body axis of a fruit fly (Insecta) and other arthropods, suggesting the molecular basis of morphological variation within the phylum. (Reprinted with permission from A. H. Knoll and S. B. Carroll, 1999. Early animal evolution: emerging views from comparative biology and geology. *Science* 284: 2129–2137. Copyright 1999 American Association for the Advancement of Science)

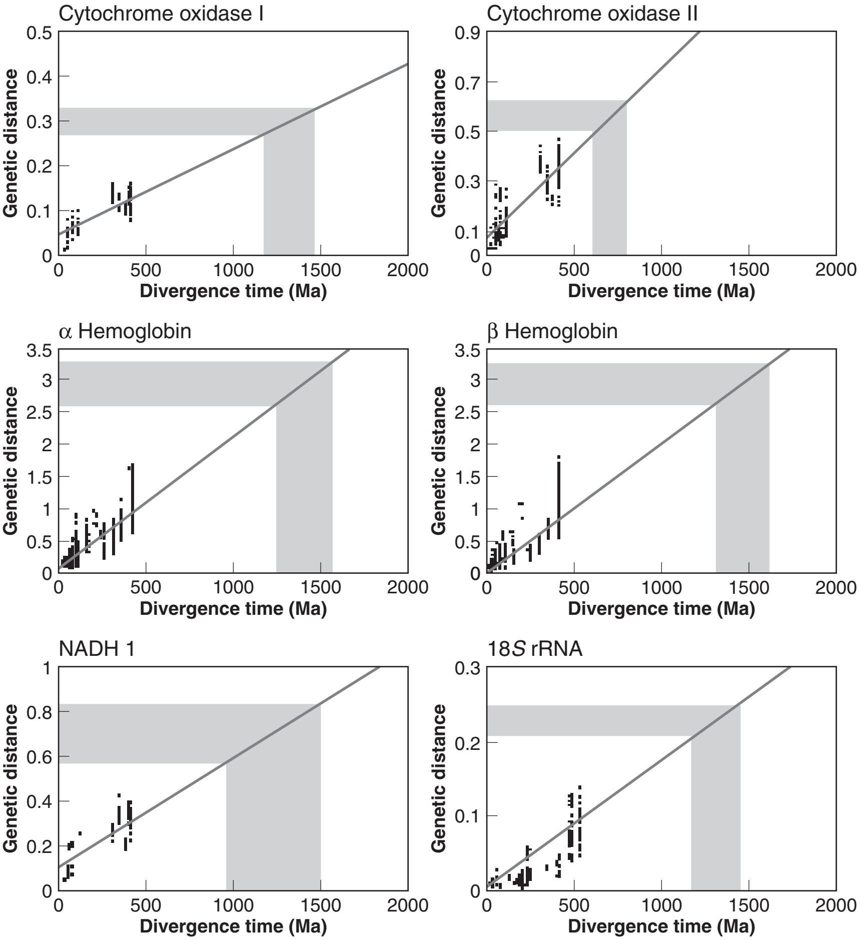

Figure 11.8. The molecular clock, illustrated using data from Wray and colleagues (1996). Shaded area shows measured genetic distances between deuterostome and ecdysozoan or lophotrochozoan species. Projection onto *x* axis estimates time since divergence from the species's last common ancestor. (Reprinted with permission from G. A. Wray, J. S. Levinton, and L. H. Shapiro, 1996. Molecular evidence for deep Precambrian divergences among metazoan phyla. *Science* 274: 568–573. Copyright 1996 American Association for the Advancement of Science)

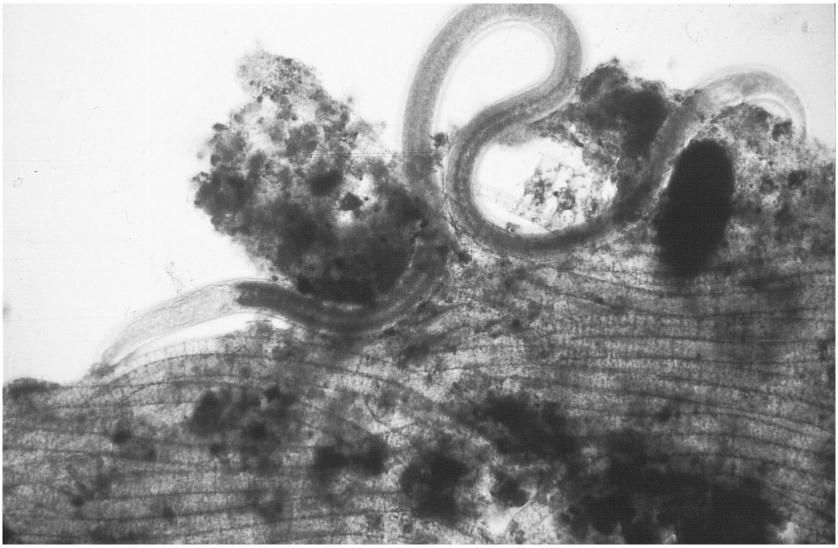

Figure 11.9. This sinuous tube, tapered at both ends, is a nematode—a tiny (less than a millimeter long) animal found almost ubiquitously in present-day environments. Nematodes have complex tissues and organs, but almost never fossilize. For comparison, the filaments in the lower part of the figure are sulfur-oxidizing bacteria! (Photo courtesy of Andreas Teske)

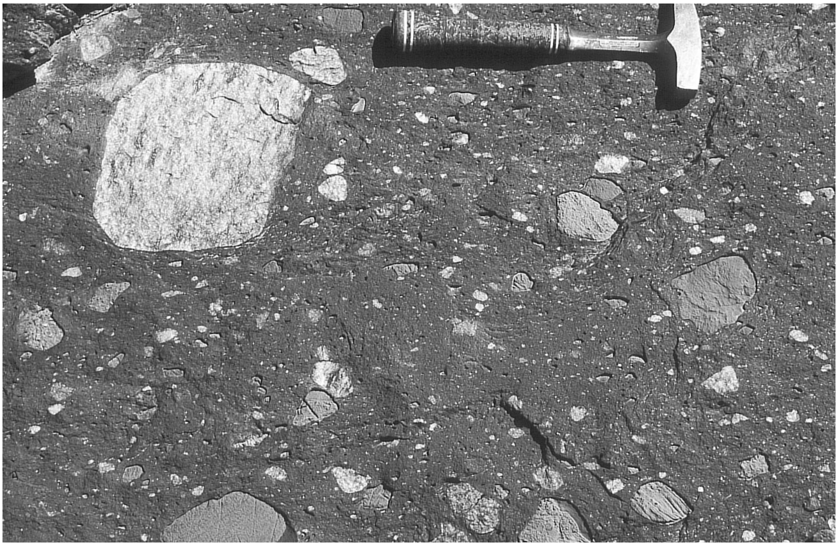

Figure 12.1. Coarse and poorly sorted sedimentary rocks of the Numees Tillite, Namibia. Similar rocks seen around the world document widespread glaciation on the late Proterozoic Earth.

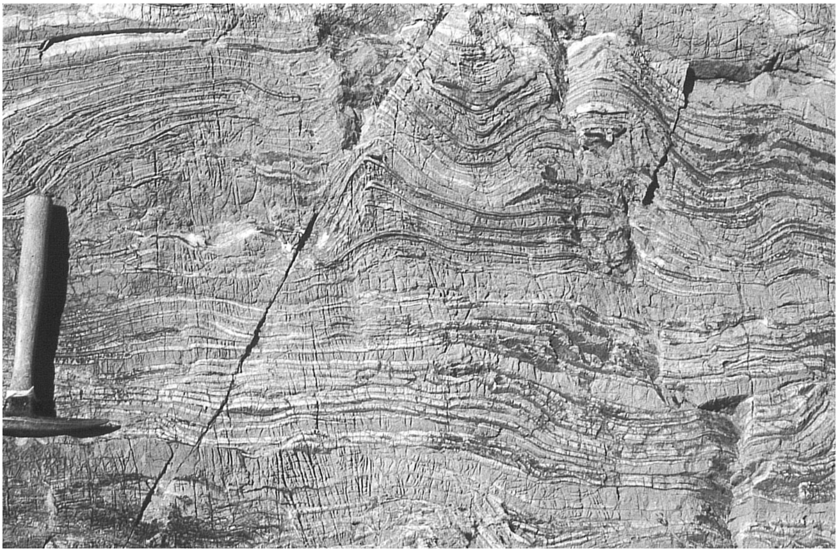

Figure 12.2. A cap carbonate above the Numees Tillite, Namibia. Cap carbonates characteristically show unusual bedding features, including the thin and contorted laminations seen here and fans of crystals deposited directly on the seafloor.

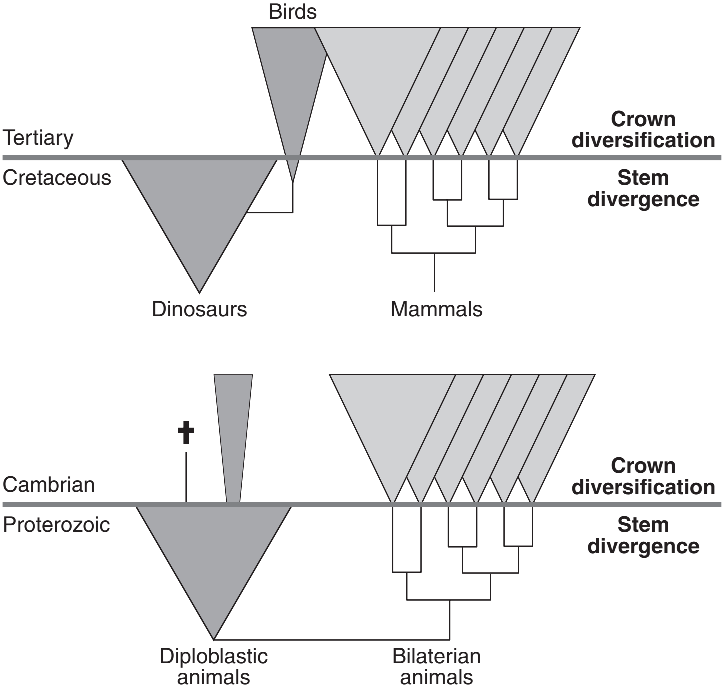

Figure 12.3. Diagram illustrating the suggested analogy between evolution on land at the Cretaceous-Tertiary boundary and evolution in the oceans at the Proterozoic-Cambrian boundary. Diploblastic animals include sponges, cnidarians, and probably, most Ediacaran organisms. (Reprinted with permission from A. H. Knoll and S. Carroll, 1999. Early animal evolution: emerging views from comparative biology and geology. *Science* 284: 2129–2137. Copyright 1999 American Association for the Advancement of Science)

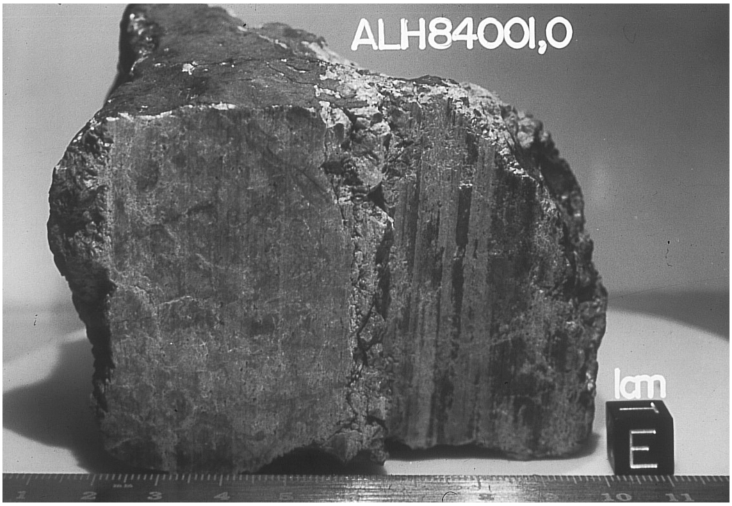

Figure 13.1. ALH-84001, the grapefruit-size meteorite from Mars that touched off debate about Martian biology. (Photo courtesy of NASA/JPL/Caltech)

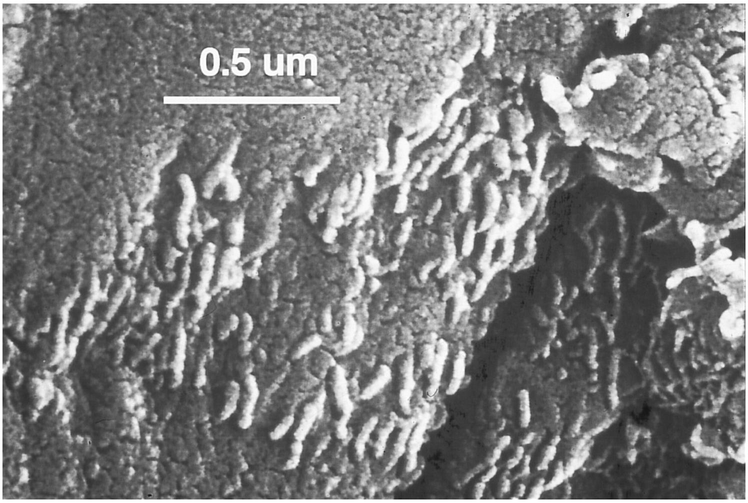

Figure 13.2. Tiny structures interpreted by David McKay and colleagues as nanofossils in ALH-84001. The longest structures are only about 100 nanometers long, not much bigger than the ribosomes found in living cells. (Photo courtesy of NASA/JPL/Caltech)

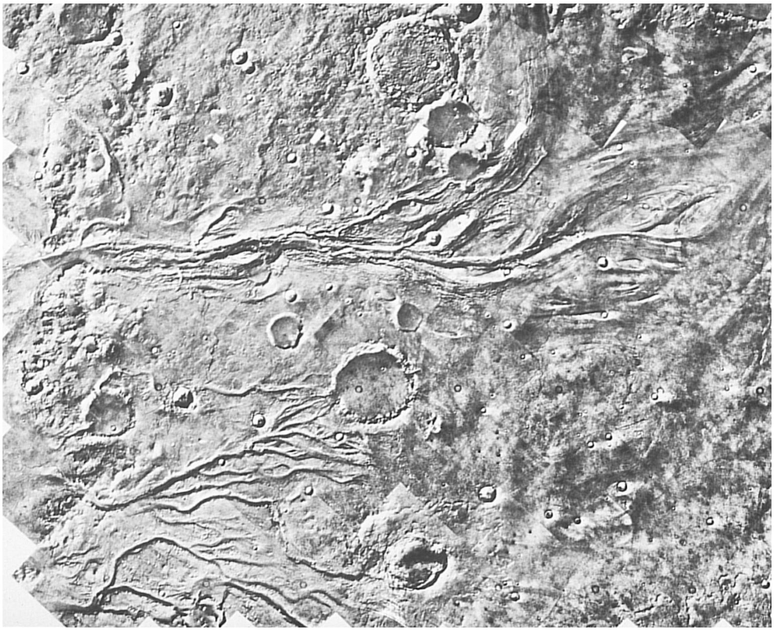

Figure 13.3. Channel network carved by water into the surface of Mars. These channels formed early in the red planet's history, principally by groundwater sapping and catastrophic melting. How much liquid water existed at any one time—whether early Mars had persistent oceans or long-lived rivers and lakes—remains a subject of debate. (Viking Image courtesy of NASA/JPL/Caltech)

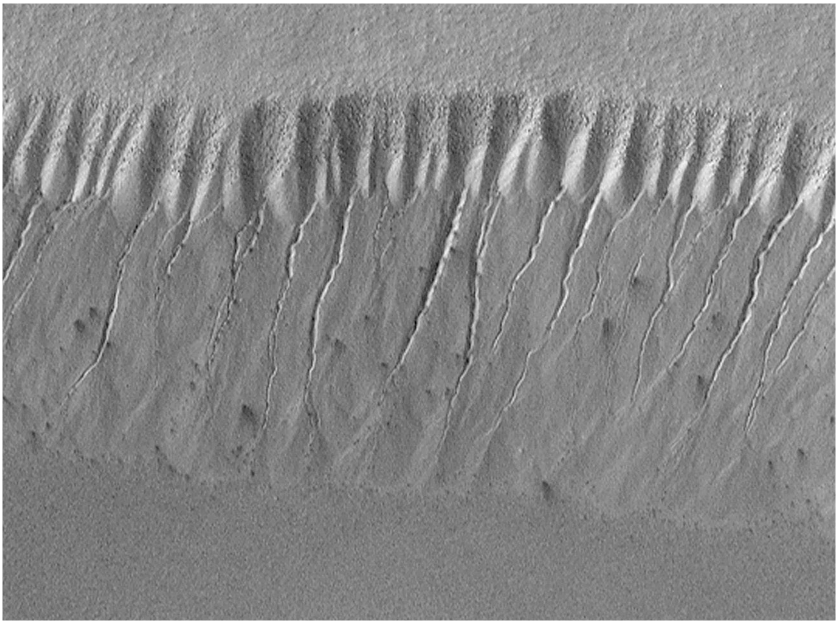

Figure 13.4. Gullies cut in relatively recent times into talus slopes beneath the walls of Martian craters. Such features suggest that liquid water can still form at the Martian surface—but how continuously it forms and how long it lasts remain uncertain. (Mars Global Surveyor Image courtesy of NASA/JPL/Malin Space Systems)